The drainage of glacier and ice sheet surface lakes: supplementary material

Christian Schoof, Sue Cook, Bernd Kulessa and Sarah Thompson

September 25, 2022

1 The reduced model and critical flux in dimensional form

For completeness, we state here the final reduced model of the main paper (equations (10)–(11) therein) in dimensional and regularized (making the water flux q unique)

$$\begin{aligned} b_t + Ub_x =& w - kcq^{3(1-\alpha)/(3-\alpha)} \max(-b_x, 0)^{3/(3-\alpha)} \\ V(h_0)_t =& q_0(t) - q \\ q =& \mathcal{Q}_s(h_0 - b_m, b_x^-, b_x^+) \end{aligned}$$

where h_0 is water level in the lake, $b_m(t) = \sup_{x>0} b(x,t)$ is seal height, b_x^- and b_x^+ are lake bed and channel slopes just up- and downstream of the seal, and q is water flux in the channel. The regularizing flux law $\mathcal{Q}_s$ is defined by the solution of boundary layer problem in sections 2.5–2.6; its key features are that $\mathcal{Q}_s$ is non-negative, vanishes when $h_0 < b_m$ and increases very rapidly first argument when $h_0 > b_m$. The function $c(x,t)$ indicates whether water is ponded or flowing at a given location, defined in rather awkward form through $c(x,1) = 1$ if $b(x,t) \geq \sup_{x'>x} b(x't)$ and $c = 0$ otherwise. The dimensional constant k is given by

$$k = \frac{\rho_w f}{8\rho\mathcal{L}} \left(\frac{8g}{fc_1}\right)^{3/(3-\alpha)}$$

and the constants ρ_w, ρ g, f, $\mathcal{L}$, c_1 and α are defined in section 2.1 of the main paper, while U and w are horizontal advection and vertical uplift velocities for the ice into which the channel is incised. The corresponding steady water inflow rate to the lake at which the seal will be breached is given by equation (31) of the main paper, again in dimensional form.

$$q_{0,crit} = \frac{\alpha^{\alpha/[3(1-\alpha)]}(3-\alpha)^{(3-\alpha)/[3(1-\alpha)]}}{3^{1/(1-\alpha)}} \left(\frac{8\rho_w\mathcal{L}}{\rho_w f}\right)^{3-\alpha/(3(1-\alpha))} \left(\frac{fc_1}{8g}\right)^{1/(1-\alpha)} U^{1/(1-\alpha)}[-\inf(w)]]^{-\alpha/[3(1-\alpha)]},$$

where (as elsewhere in this paper) we have assumed that U is constant.

Note that, in the above, we have used a self-similar relationship between cross-sectional area and wetted perimeter of the channel in the form

$$P(S) = c_1 S^\alpha$$

In section 2 below, we revisit the formulation of the reduced model above, relaxing our assumptions on the relationship between wetted perimeter, water depth and cross-sectional area.

2 The formulation of the reduced model

2.1 The full model restated

We begin with the dimensionless full model,

$$\delta S_t + (uS)_x = \varepsilon u^3 P(S), \tag{1a}$$

$$\nu Fr^2 S(\delta u_t + u u_x) = -u^2 P(S) - S b_x - \nu S h(S)_x, \tag{1b}$$

$$b_t + U b_x = w - u^3. \tag{1c}$$

For completeness, we also define an unincised ice surface elevation through $us_x = w$, and note that $b \leq s$ throughout. As in the main paper, we assume that $\delta \ll 1$, $\nu \ll 1$ and $\varepsilon \ll 1$. In order to deal with ponded sections in section 2.2, we tighten the restriction on δ to be $\delta \ll h^{-1}(\nu^{-1})$, where h^{-1} is the inverse of the water depth function h. The appropriate leading order model is

$$(uS)_x = 0, \qquad u^2 P(S) = -S b_x, \qquad b_t + U b_x = w - u^3. \tag{2}$$

From this, we obtain the same reduced model as in the main paper

$$b_t + U b_x + c M(-b_x, q) = w \tag{3}$$

where flux $q = uS$ is independent of x, and the ponding function c is

$$c(x,t) = \begin{cases} 0 & \text{if } b(x,t) < \sup_{x'>x} b(x',t), \\ 1 & \text{otherwise.} \end{cases} \tag{4}$$

as demonstrated in section 2.2.

The definition of c ensures that $c(x,t)M(-b_x, q) = 0$ if $b_x > 0$, and we can set $M(-b_x, q) = 0$ if $-b_x < 0$, and we likewise demand that $M(-b_x, q) = 0$ if $q = 0$, while for $-b_x \geq 0$, $q > 0$, M is defined implicitly through

$$M = u^3, \qquad \frac{u^3}{q} P\left(\frac{q}{u}\right) = -b_x. \tag{5}$$

We will assume below that $P : [0, \infty) \mapsto [0, \infty)$ is a non-decreasing, (strictly) concave function, differentiable except possibly at the origin, with $P(S) > 0$ if $S > 0$. Then $M(-b_x, q)$ is (strictly) convex and increasing in $-b_x$ for $-b_x \geq 0$, and non-decreasing in q. If P lacks concavity but hydraulic radius

$$f(S) = S/P(S)$$

is an increasing function of S with $f(0) = 0$, then M is at least an increasing function of $-b_x$, and a non-decreasing function of q. In both cases, $M(0, q) = 0$ for $q > 0$.

To demonstrate this, assume $q > 0$. Note first that for a non-negative, concave function P, $P'(S) \leq P(S)/S$ follows from the mean value theorem, with $P'(S) < P(S)/S$ for strictly concave P. Consequently, $f(S) = S/P(S)$ is a non-decreasing function of S either by assumption, or due to concavity. As a result, $1/f(S) = P(S)/S$ is a non-increasing function of S, and hence $1/f(q/u) = (u/q)P(q/u)$ is non-decreasing and non-zero for $u > 0$. With that in hand, differentiate the left-hand side of $(5)_2$,

$$g(u, q) = \frac{u^3}{q} P\left(\frac{q}{u}\right),$$

with respect to u for $u > 0$:

$$g_u = \frac{3u^2}{q} P\left(\frac{q}{u}\right) - u P'\left(\frac{q}{u}\right) \tag{6}$$

With $P'(q/u) \leq P(q/u)u/q$, the right-hand side is clearly positive, and bounded below by $2u/f(u/q)$, which itself is bounded below away from zero except possibly near $u = 0$. Since $1/f(q/u)$ is non-decreasing in u as well as positive, it remains bounded as $u \to 0$ from above, and it follows that $g(u, q) = u^2/f(q/u) \to 0$ as $u \to 0$, in addition to $g_u > 0$ for all positive u. Hence $(5)_2$ has a unique, positive solution for all $-b_x \geq 0$, with $u = 0$ when $-b_x = 0$. It follows that $M(0, q) = 0$. We also have

$$-\frac{\partial u}{\partial b_x} = \frac{1}{g_u}, \tag{7}$$

where we have just demonstrated that the right-hand side is positive. Hence $M_{-b_x}(-b_x, q) = -3u^2\partial u/\partial b_x \geq 0$, with $M_{-b_x}(-b_x, q) > 0$ if $-b_x > 0$; melt rate M increases with downward slope $-b_x$. Similarly,

$$g_q = -\frac{u^3}{q^2}P\left(\frac{q}{u}\right) + \frac{u^3}{q^2}\frac{q}{u}P'\left(\frac{q}{u}\right) \leq 0,$$

Hence, since $P'(S) \leq P(S)/S$,

$$\frac{\partial u}{\partial q} = -\frac{g_q}{g_u} \geq 0$$

and therefore $M_q \geq 0$; $M_q > 0$ for $-b_x > 0$ and $q > 0$ if P is strictly concave or hydraulic radius $f(S)$ is an increasing function of S.

To prove (strict) convexity for (strictly) concave P, note that we have to show that $M_{-b_x}(-b_x, q)$ is non-decreasing (increasing) with increasing $-b_x$. Once more, we have

$$M_{-b_x}(-b_x, q) = \frac{3u^2}{\frac{3u^2}{q}P\left(\frac{q}{u}\right) - uP'\left(\frac{q}{u}\right)} = \frac{3q}{3P\left(\frac{q}{u}\right) - \frac{q}{u}P'\left(\frac{q}{u}\right)}. \tag{8}$$

where u is defined through (5), and we know that u increases with $-b_x$. If P is (strictly) concave and non-decreasing, $P(S) - SP'(S)$ is an non-decreasing (increasing) function of S, and hence $P(q/u) - q/uP'(q/u)$ is a non-increasing (decreasing) function of u, while the same is true of $P(q/u)$ itself. Hence the denominator on the right of (8) is non-increasing (decreasing), and M_{-b_x} is non-decreasing (increasing), proving (strict) convexity.

Note that the model (3) is solved numerically in the main paper for specific, concave power laws $P(S) = S^\alpha$, $h(S) = S^\beta$ for $0 \leq \alpha < 1$, $0 < \beta \leq 1$. We also assume these constitutive relations for P and h in the appendices of the main paper for the analysis of the boundary layers that occur in the full model (10) at shocks and discontinuities in c of the reduced model (3). Note that a power-law P as specified satisfies the constraints defined earlier in the present section.

We stress that the abstract analysis and numerical method of solving equation (3) in the main paper only assumes the properties for M that we have established here for concave P above: convexity, monotonicity in $-b_x$ and q, and vanishing M at $-b_x = 0$. In addition, that analysis and numerical method assume that the ponding function in (4) is correctly defined, and that there is continuity of b at shocks and discontinuities in c..

The purpose of the remainder of the remainder of section 2 of these supplementary notes is to justify these last two assumptions — the definition of c, and continuity of b and its implications for shocks and discontinuities in c — for more general constitutive relations. Here, we generalize the analysis of ponded sections and of boundary layers in the main paper to more general functions P and h, just as we have already done in determining the properties of M above. In addition to the constraints on P that we have already defined, we will further take $h : [0, \infty) \mapsto [0, \infty)$ to be an unbounded, increasing function, differentiable except possibly at the origin, satisfying $h(0) = 0$. We show that, with these general constraints on P and h, the qualitative properties of the boundary

layers analyzed in the appendices to the main paper remain unchanged, thus justifying the treatment of shocks and discontinuities in c in the main paper for these ore general constitutive relations.

Section 3 provides a brief analysis of instabilities that occur above a critical Froude number, followed by a section that provides further justification for the seal breach criteria derived in the main paper, and a section detailing the numerical method used to compute solutions in the main paper as well as a number of additional computation solutions that supplement those shown in the main paper.

2.2 The ponded region

As we have just described, the main challenges in taking the model (3) at face value is the appearance of the ponding function c, the nature of shocks and expansion fans that arise in the absence of that ponding function, and those that result from discontinuities in c. We address these issues in turn, dealing first with ponded sections and the definition of the ponding function.

The rescaling of (1) relevant to a ponded area is

$$S = h^{-1}\left(\nu^{-1}\right)\hat{S}, \qquad u = \hat{u}/h^{-1}\left(\nu^{-1}\right), \tag{9}$$

for general monotone functions h with inverse h^{-1}, provided the function h is unbounded and $h^{-1}(\nu^{-1})$ therefore exists as $\nu \to 0$. With (9) the model (1) becomes

$$\delta h^{-1}(\nu^{-1})\hat{S}_t + \left(\hat{S}\hat{u}\right)_x = \frac{\varepsilon P(h^{-1}(\nu^{-1}))}{[h^{-1}(\nu^{-1})]^3}\hat{u}^3 \tag{10a}$$

$$\frac{Fr^2}{h^{-1}(\nu^{-1})}\hat{S}\left(\delta\hat{u}_t + \frac{1}{h^{-1}(\nu^{-1})}\hat{u}\hat{u}_x\right) = -\frac{P(h^{-1}(\nu^{-1}))}{[h^{-1}(\nu^{-1})]^3}\hat{u}^2\hat{P}\left(\hat{S}\right) - \hat{S}\left[b + \hat{h}(\hat{S})\right]_x \tag{10b}$$

$$b_t + Ub_x = w - \frac{1}{[h^{-1}(\nu^{-1})]^3}\hat{u}^3 \tag{10c}$$

where

$$\hat{h}(\hat{S}) = \nu^{-1}h(h^{-1}(\nu^{-1})\hat{S}) = \nu^{-1}h(S) \qquad \hat{P}(\hat{S}) = P(h^{-1}(\nu^{-1})\hat{S})/P(h^{-1}(\nu^{-1})) \tag{11}$$

are $O(1)$ function of $\hat{S}$. The above is hard to read: for $\nu \ll 1$ and h a monotonically increasing, unbounded function, $h^{-1}(\nu^{-1}) \gg 1$ is large. We make the same assumption as in the main paper, that hydraulic radius $S/P(S)$ is an increasing function of S, and hence $P(S) = O(S)$ or smaller for large S. Consequently

$$\frac{P(h^{-1}(\nu^{-1}))}{[h^{-1}(\nu^{-1})]^3} \ll 1. \tag{12}$$

and the last term in (10b) dominates.

At this point, we also tighten our assumptions on δ and ν to $\delta h^{-1}(\nu^{-1}) \ll 1$ and $\nu \ll 1$. The mass storage term $\delta h^{-1}(\nu^{-1})$ in (10a) then does not appear at leading order, and flux q remains constant as assumed above in (3). At leading order, (10) becomes

$$\left(\hat{u}\hat{S}\right)_x = 0, \qquad \left(b + \hat{h}\right)_x = 0, \qquad b_t + Ub_x = w \tag{13}$$

Equation $(13)_3$ is indeed (3) with $c = 0$; the only issue is making sure that c is correctly defined.

From $(13)_2$, the surface elevation defined by $\hat{h}_w = b + \hat{h}$ remains constant. Matching with the flowing section on the far side of the dowstream seal occurs through a boundary layer in which $h \sim O(1)$, $\hat{h} = O(\nu)$ while $hu =$ constant at leading order as described in section 2.5, and the same

is true at the upstream end of a ponded section (section 2.7). Consequently, $\hat{h} \to 0$, $\hat{S} \to 0$ at the ends of a ponded section at leading order in order to match to the flowing sections, while $\hat{u}\hat{S} = q$ remains constant at leading order. Hence b takes the same value at both ends of the ponded section, and (since $\hat{h} > 0$), b is below that value inside the ponded section. Since we must have $b_x < 0$ in any flowing section then, with $q > 0$, the ponded section must terminate at a local maximum of b. The definition $\{x : b(x,t) < \sup_{x'>x} b(x',t)\}$ for the union of ponded sections follows, as does the ponding function c in equations (3).

2.3 Boundary layers

The need to investigate boundary layers arises from three distinct situations. First, for a nonlinear melt rate M, shocks can form spontaneously in solutions to (3); that equation itself ceases to hold in strong form at such shocks, and an additional closure for the movement of the shock is required. A boundary layer treatment of the full model in principle provides that closure (although as shown in the main paper, the same result as we obtain in section 2.4 is arrived at if we simply assume that the solution remains continuous across the shock.

Second, a shock also forms where a ponded section exists upstream of a flowing section, which we investigate in section 2.5, only to find that again the shock moves in the way required by continuity of b across the shock. In section 2.6, we investigate how the water level difference between ponded section and seal height can be computed, demonstrating that this water level difference indeed remains a higher order correction.

Third, the transition from flowing to ponded corresponds either to a simple jump in slope b_x, or to an expansion fan as already discussed in the main paper. We generalize the results presented there to generic functions P and h in section 2.7.

These shocks were already analyzed in the main paper, where we restricted ourselves to $P(S) = S^\alpha$, $h(S) = S^\beta$. Here, we generalize those assumptions to show that the same results hold if we assume that $P(S)$ is a non-decreasing, concave function with $P(0) = 0$, and $h(S)$ is an unbounded, monotonically increasing function, with P and h continuously differentiable except possibly at $S = 0$. We also provide additional detail on the conclusion in the appendices of the main paper that channel base elevation b and water surface elevation $b + h(S)$ are continuous across shocks at leading order.

2.4 The shock boundary layer

A shock forms where the bed slope steepens discontinuously in (3). In the full scaled model (1), that steepening is not discontinuous but occurs over a short length scale $\sim \nu$. Assuming that the shock is at a moving location $x = x_c(t)$, the appropriate rescaling is

$$X = \frac{x - x_c(t)}{\nu}, \qquad T = t, \qquad B = \frac{b(x,t) - b_0\left(x_c(t)^-, t\right)}{\nu}, \qquad \Sigma = S, \qquad V = u, \tag{14}$$

where b_0 is the outer solution satisfying (3), and the superscript '$-$' denotes the limit taken as x_c is approached from below. We will likewise use the superscript '$+$' for the limit taken from above. Under this rescaling, we obtain the following leading-order problem for $\Sigma(X,T)$, $V(X,T)$ and $B(X,T)$:

$$(V\Sigma)_X = 0 \tag{15a}$$

$$Fr^2 \Sigma V V_X = -V^2 P(\Sigma) - \Sigma B_X - \Sigma h(\Sigma)_X, \tag{15b}$$

$$b_{0,t}^- + b_{0x}^- \dot{x}_c + (U - \dot{x}_c) B_X = w(x_c) - V^3, \tag{15c}$$

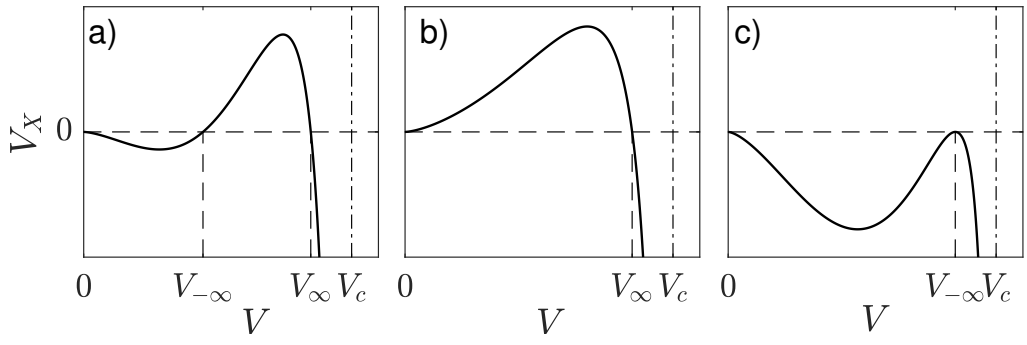

Figure 1: V_X in the boundary layer as defined by equation (17) for a shock in a flowing sectiom (panel a), equation (22b) for a shock at the downstream end of a ponded section (panel b) and equation (17) for the upstream end of a ponded section (panel c). $h(S) = P(S) = S^{1/2}$, $Fr = 0.575$ and $q = 1$ in each case, with $b_x^- = -.2$, $b_x^+ = -1$ (panel a), $b_x^- = 1$, $b_x^+ = -1$ (panel b) and $b_x^- = -1$, $b_x^+ = \alpha b_x^-/3$ (panel c), the latter being the critical upstream slope generated by an expansion fan, at which the weak inequality (45) becomes an equality. For smaller slopes b_x^-, the repeated root of V_X at $V_{-\infty}$ splits into two distinct roots, the smaller of which is the flow velocity $V_{-\infty}$ upstream of the pond entry point. $V_{-\infty}$ and V_∞ are defined in the text, V_c is the Froude critical velocity defined by $Fr^2V^3/[qh'(q/V)] = 1$.

where the dot denotes differentiation with respect to time t. Matching with the upstream far field, we obtain using $(2)_3$ that $V\Sigma = q$ and $b_{0t}^- = w(x_c) - Ub_{0x}^- - V_{-\infty}^3$, where $V_{-\infty} = \lim_{X\to-\infty} V = u(x_c(t)^-, t)$.

Eliminating Σ and substituting for b_{0t}^-

$$Fr^2qV_X = -V^2P\left(\frac{q}{V}\right) - \frac{q}{V}B_X - \frac{q}{V}h\left(\frac{q}{V}\right)_X \tag{16a}$$

$$(U - \dot{x}_c)B_X = -(U - \dot{x}_c)b_{0x}^- - V^3 + V_{-\infty}^3 \tag{16b}$$

Here we consider a shock connecting two flowing sections satisfying (2), so $c = 1$ on both sides of the shock in (3). Hence $V_{-\infty}$ satisfies the far field equation $(2)_2$, $V_{-\infty}^2P(qV_{-\infty}^{-1}) = -qV_{-\infty}^{-1}b_{0x}^-$. Consequently, then writing b_{x0}^- in terms of $V_{-\infty}$, (16b) becomes

$$(U - \dot{x}_c)B_X = \frac{(U - \dot{x}_c)V_{-\infty}^3}{q}P\left(\frac{q}{V_{-\infty}}\right) - V^3 + V_{-\infty}^3 \tag{16c}$$

Eliminating B_X and rearranging, we find

$$V_X = \left[1 - Fr^2\frac{V^3}{qh'\left(\frac{q}{V}\right)}\right]^{-1}\frac{V^2}{qh'\left(\frac{q}{V}\right)}\left[\frac{V^3}{q}P\left(\frac{q}{V}\right) - \frac{V_{-\infty}^3}{q}P\left(\frac{q}{V_\infty}\right) - \frac{V^3 - V_{-\infty}^3}{U - \dot{x}_c}\right], \tag{17}$$

where the prime on h' denotes an ordinary derivative. The solution to (17) needs to connect the upstream far-field $V_{-\infty}$ to a downstream far-field $V \to V_\infty$ as $X \to \infty$, where $V_\infty^2P(qV_\infty^{-1}) = -qV_\infty^{-1}b_{0x}^+$ (figure 1a). Since we assume a shock connecting two flowing sections, we have $V_\infty > 0$.

Subcriticality implies that V remains small enough to ensure that

$$Fr^2\frac{V^3}{qh'\left(\frac{q}{V}\right)} < 1. \tag{18}$$

We assume that $V^3/h'(q/V)$ is monotone in V, and vanishes as $V \to 0$; the latter implies that $h'(\Sigma) \gg \Sigma^{-3}$ for large Σ, which turns out to be necessary if h is an unbounded function as assumed in section 2.2. With these assumptions in place, subcriticality corresponds to V being less than some threshold, as in the standard St Venant equations.

We assume that P is strictly concave as well as satisfying the other constraints in section 2.1, so the melt rate $M(-b_x, q)$ in the outer model is strictly convex; as shown in the main paper, a treatment of the shock assuming continuity of the outer solution b_0 across the shock then ensures that characteristics indeed enter it from both sides. If P is indeed strictly concave, it can be shown that the V-derivative of the second square bracket in (17) changes sign at most once, from positive to negative, and therefore has at most two roots. These roots, along with $V = 0$, are the fixed points of (17). Specifically, that derivative is

$$\frac{V^2}{q}\left[3P\left(\frac{q}{V}\right) - \frac{q}{V}P'\left(\frac{q}{V}\right) - \frac{3}{U - \dot{x}_c}\right] \tag{19}$$

As in the analysis of (8), strict concavity implies that $P(q/V) - q/VP(q/V)$ is a decreasing function of V, while $P(q/V)$ also decreases with V; hence the the square bracket in (19) is a decreasing function of V and the desired result follows.

Matching the downstream far-field $V \to V_\infty$ requires V_∞ to be the larger, stable of the two roots, with $V_{-\infty}$ the smaller, unstable root. In order for V_∞ to be an equilibrium of V, we require

$$\frac{V_\infty^{3-\alpha} - V_{-\infty}^{3-\alpha}}{q^{1-\alpha}} - \frac{V_\infty^3 - V_{-\infty}^3}{U - \dot{x}_c} = 0,$$

to hold, or alternatively, using the relationship between $V_{\pm\infty}$ and $b_{0x}^{\pm}$, and the definition of M,

$$\dot{x}_c = U - \frac{q(V_\infty^3 - V_{-\infty}^3)}{V_\infty^3 P\left(\frac{q}{V_\infty}\right) - V_{-\infty}^3 P\left(\frac{q}{V_{-\infty}}\right)} = U + \frac{M(-b_{0x}^+, q) - M(-b_{0x}^-, q)}{b_{0x}^+ - b_{0x}^-} \tag{20}$$

as derived in the main paper for a shock at which b is continuous. In order for V_∞ to be the larger root, we also require that $b_{0x}^+ < b_{0x}^-$.

Lastly, we can confirm that b is indeed continuous at leading order across the boundary layer, and in fact, we can choose the location x_c to make the outer solution b_0 continuous. In fact, the boundary layer problem is invariant under a shift in X, and we can make the solution unique as a function of X by demanding that the outer bed elevation is strictly continuous with $b_0^- = b_0^+$. From the definition of B, we have $b(x,t) = b_0^- + \nu B(X)$. In the upstream matching region, where $x \to 0^-$, $X \to -\infty$, we require $b_0^- + \nu B(X) \sim b_0^- + b_{0x}^-(x - x_c) = b_0^- + \nu b_{0x}^- X$, or $B(X) - b_0^- X \to 0$. Downstream, as $x \to 0^+$, $X \to \infty$, matching of bed elevation requires $b_0^- + \nu B(X) \sim b_0^+ + b_{0x}^+(x - x_c) = b_0^+ + \nu b_{0x}^+ X$. Hence $b_0^+ - b_0^- = \nu \lim_{X\to\infty}\left(B(X) - b_{0x}^+ X\right)$, which we can write as

$$b_0^+ - b_0^- = \nu\left(\int_0^\infty B_X(X) - b_{0x}^+ \mathrm{d}X + \int_{-\infty}^0 B_X(X) - b_{0x}^- \mathrm{d}X\right). \tag{21}$$

The integral is finite when the second square bracket in (17) has two distinct roots, with B_X supplied by (16c) approaching the far field values $b_{0x}^{\pm}$ exponentially in X. Hence the jump in b_0 is of $O(\nu)$, which we can interpret as a matter of precisely locating the shock x_c: by a shift of the origin X, we can ensure that the sum of integrals above is in fact zero.

2.5 The seal downstream of a ponded section

As in the main paper, the generalization to a solution that connects a ponded section upstream to a flowing section downstream is straightforward. Again, the relation $V_{-\infty}^2 P(qV_{-\infty}^{-1}) = -qV_{-\infty}^{-1} b_{0x}^-$ ceases to hold, and we obtain instead

$$B_X = b_{0x}^- - \frac{V^3}{U - \dot{x}_c} \tag{22a}$$

$$V_X = \left[1 - Fr^2 \frac{V^3}{qh'\left(\frac{q}{V}\right)}\right]^{-1} \frac{V^2}{qh'\left(\frac{q}{V}\right)} \left[\frac{V^3}{q} P\left(\frac{q}{V}\right) + b_{0x}^- - \frac{V^3}{U - \dot{x}_c}\right]. \tag{22b}$$

The solution must connect $V = 0$ upstream to a finite $V_\infty > 0$ downstream, satisfying $V_\infty^2 P(qV_\infty^{-1}) = -qV_\infty^{-1} b_{0x}^+$ (figure 1b). We assume as before that V_∞ is subcritical, so (18) holds. Again, V_∞ must be an equlibrium of (22), so

$$b_{0x}^- + \frac{V_\infty^3}{q} P\left(\frac{q}{V}\right) - \frac{V_\infty^3}{U - \dot{x}_c} = 0, \tag{23}$$

or, again using the relationship between V_∞ and b_{0x}^+ and the definition of M,

$$\dot{x}_c = U - \frac{V_\infty^3}{b_{0x}^- + q^{-1} V_\infty^3 P\left(\frac{q}{V_\infty}\right)} = U + \frac{M(-b_{0x}^+, q)}{b_{0x}^+ - b_{0x}^-}. \tag{24}$$

This is the same as the jump condition derived in the main paper on the basis of continuity in b. We elaborate further on continuity of b in the next subsection. We can also demonstrate that the fixed point V_∞ is stable if $b_{0x}^- > 0$, since if $F(V) = V^3/qP(q/V) + b_{0x}^- - V^3/(U - \dot{x}_c)$ and $F(V_\infty) = 0$, then $F'(V_\infty) = 3(F(V_\infty) - b_{0x}^-)/V_\infty - V_\infty P'(q/V_\infty) = -3b_{0x}^-/V_\infty - VP'(q/V) < 0$, P being an increasing function. By the same argument as that made following (17), it follows that V_∞ is the only non-zero fixed point of (22): the second square bracket in (22) admits at most two roots, one stable and one unstable, and we have just shown that with $b_{0x}^- > 0$, there can only be a stable root. Hence there exists a solution of (22) connecting $V = 0$ to $V = V_\infty$.

Note that we require $b_{x0}^+ < 0$, $V_\infty > 0$ for a solution. In addition, in order to match the upstream conditions of $V \to 0$ as $X \to -\infty$, we require the integral

$$\int \frac{qh'\left(\frac{q}{V}\right)}{V^2} \mathrm{d}V = -\int h'(\Sigma) \mathrm{d}\Sigma$$

to diverge as the lower limit of integration in V goes to 0, or equally the upper limit of integration in $\Sigma = q/V$ goes to infinity. This is nothing more than the requirement that h be unbounded, as previously stipulated for the model of the ponded section in section 2.2.

2.6 Continuity of elevation and water level above the seal

As in (21), we can again show that bed elevation remains continuous at leading order in the seal boundary layer of section 2.5, with some caveats regarding the order of the leading correction term. The difference with the calculation in the previous section is that B_X no longer has to approach b_{0x}^- exponentially in X in the upstream matching region:

$$B_X - b_{0X}^- = \frac{V^3}{U - \dot{x}_c} = \frac{q^3}{(U - \dot{x}_c)\Sigma^3}, \tag{25}$$

and we require that V^3 (or $1/\Sigma^3$) be integrable in X in order for the right-hand integral $\int_{-\infty}^{0} B_X(X) - b_{0x}^- \mathrm{d}X = \int V^3/(U-\dot{x}_c)\mathrm{d}X$ in (21) to exist. We can test this by changing to V as the variable of integration: as $X \to -\infty$, $V \to 0$, and $X_V = 1/V_X \sim qh'(q/V)/(b_{0x}^- V^2)$. Hence we obtain an integral of the form

$$\int \frac{V^3}{U-\dot{x}_c} \frac{qh'\left(\frac{q}{V}\right)}{b_{0x}^- V^2} \mathrm{d}V = \int \frac{q^3}{(U-\dot{x}_c)b_{0x}^-} \frac{h'(\Sigma)}{\Sigma^3} \mathrm{d}\Sigma$$

where $\Sigma = q/V$. The integral exists when the lower limit in V goes to zero provided $V^3 h'(q/V)/V^2 = Vh'(q/V)$ is integrable down to $V = 0$, or equivalently, if if $h'(\Sigma)/\Sigma^3$ is integrable as $\Sigma \to \infty$. This is certainly true of the power law $h(S) = S^\beta$ with $0 < \beta \leq 1$ used in the main paper. We revisit the case where the integral does not converge below, which requires higher-order matching with the ponded solution of section 2.2.

Before we develop that ponded solution to higher order, we consider how to compute water level: the leading-order outer model of section 2.2 relies on there being no jump in water surface elevation at the downstream end of a ponded section. In order for that to be the case, any deviation of water level in a ponded section from the downstream seal height must be higher order correction.

For definiteness, we ensure a unique solution as at the end of section 2.4 by ensuring that $b_0^+ = b_0^-$ to an error of $o(\nu)$, and choose $x = x_c$, $X = 0$ to coincide with that position. Water surface elevation in the boundary layer is at $h_w := b + \nu h(S) = b_0^- + \nu(B + h(\Sigma))$, and we are ultimately interested in computing the difference between water level in the ponded region $\hat{h}_w$ and the 'outer' seal height b_0^-, since our model for the ponded region is based on $\hat{h}_w - b_0^- \ll 1$.

Defining $H_w = (h_w - b_0^-)/\nu$, we have

$$H_{w,X} = B_X + h'(\Sigma)\Sigma_X = B_X - \frac{q}{V^2} h'\left(\frac{q}{V}\right) V_X \tag{26}$$

water level above the seal is therefore

$$H_w(X,T) = h(\Sigma(0,T)) - B(0,T) - \int_X^0 B_X + h'(\Sigma)\Sigma_X \mathrm{d}X = h(\Sigma(0,T)) - \int_X^0 B_X - \frac{q}{V^2} h'\left(\frac{q}{V}\right) V_X \mathrm{d}X'. \tag{27}$$

Here the integrand is a function of (X', T), and can be computed using(22) and (24).

Key is the behaviour of the integrand as $X \to -\infty$, $V \to 0$. Using (22), we have

$$H_{w,X} \sim -\frac{V^3}{q} P\left(\frac{q}{V}\right) - \frac{Fr^2 V^3}{qh'\left(\frac{q}{V}\right)} b_{0x}^- = -\frac{q^2}{\Sigma^3} P(\Sigma) - \frac{Fr^2 q^2}{\Sigma^3 h'(\Sigma)} b_{0x}^-. \tag{28}$$

H_w remains finite if the integral (27) converges as $X \to -\infty$, which corresponds to $V \to 0$, $\Sigma = q/V \to \infty$. As above,from (22), we have $X_V \sim qh'(q/V)/(b_{0x}^- V^2)$ at small V, or equally $X_\Sigma \sim -h'(\Sigma)/b_{0x}^-$ as $\Sigma \to \infty$. The second term in each expression for $H_{w,X}$ in (28) then leads to an integral of the form

$$\int -\frac{Fr^2 V^3}{qh'\left(\frac{q}{V}\right)} b_{0x}^- \mathrm{d}X = \int -Fr^2 V \mathrm{d}V = \int \frac{Fr^2 q^2}{\Sigma^3} \mathrm{d}\Sigma, \tag{29}$$

which remains finite as the lower limit of integration in V goes to zero, or equally the upper limit of integration in Σ goes to infinity. The first term meanwhile leads to an integral of the form

$$\int -\frac{V^3}{q} P\left(\frac{q}{V}\right) \frac{q}{V^2} h'\left(\frac{q}{V}\right) \mathrm{d}V = \int \frac{q^2}{\Sigma^3} P(\Sigma) h'(\Sigma) \mathrm{d}\Sigma. \tag{30}$$

In order for this integral remain finite as the lower limit in V goes to zero, or the upper limit in Σ goes to infinity, requires $P(\Sigma)h'(\Sigma)/\Sigma^3$ to be integrable. This stipulation is stronger than (12), which states that $P(\Sigma)/\Sigma^3 \ll 1$ for large Σ, but is satisfied for the power laws used in the main paper: there ,$P(\Sigma) = \Sigma^\alpha$, $h(\Sigma) = \Sigma^\beta$ with $0 \leq \alpha < 1$, $0 < \beta \leq 1$. When $P(\Sigma)h'(\Sigma)/\Sigma^3$ is integrable as described, the leading order water level correction relative to the seal is simply given by $\lim_{x\to x_c} \hat{h}_w = b_0^- + \lim_{X\to-\infty} H_w(X,T)$.

Note that the water level correction we compute will be a function of the parameters in the boundary layer model above, specifically of q, b_{0x}^- and b_{0x}^+. In other words, we expect that we can ultimately express flux q as a function of the difference between the outer water level $\lim_{x\to x_c} \hat{h}_w - b_0^-$ as well as of the slopes b_{0x}^- and b_{0x}^+.

When $P(\Sigma)h'(\Sigma)/\Sigma^3$ is not integrable, the non-integrable term corresponds to the near-seal behaviour of a higher order term in the outer solution. The same is true for the non-integrable term in the computation of B at the start of this subsection if $h'(\Sigma)/\Sigma^3$ is not integrable. In both cases, this means that the water level and bed elevation correction term remains of higher order at the outer scale. In order to deal with these non-integrable boundary layer solutions, we therefore develop a higher-order solution to (10).

For simplicity, consider the distinguished limit $Fr^2 \sim P(h^{-1}(\nu^{-1}))/h^{-1}(\nu^{-1}))$. In that case, we define

$$\mu = \frac{P(h^{-1}(\nu^{-1})}{h^{-1}(\nu^{-1})^3}.$$

Note that we can crudely relate the size of μ to ν based on whether $P(\Sigma)h'(\Sigma)/\Sigma^3$ is integrable or not: for large Σ, suppose that $h'(\Sigma) \sim h(\Sigma)/\Sigma$. Noting that integrability requires that $P(\Sigma)h'(\Sigma)/\Sigma^3 \ll \Sigma^{-1}$, this suggests that if we look at $\Sigma \sim h^{-1}(\nu^{-1})$, then integrability demands that

$$\frac{P(h^{-1}(\nu^{-1}))\nu^{-1}}{[h^{-1}(\nu^{-1})]^4} \ll \frac{1}{h^{-1}(\nu^{-1})},$$

or

$$\mu \ll \nu.$$

We expand as

$$\hat{S} = \hat{S}_0 + \mu\hat{S}_1 + \nu\tilde{S} + o(\mu) + o(\nu),$$

where the term $\nu\tilde{S}$ is a constant that is necessary in order to match the boundary layer. Similarly, $\hat{u} = \hat{u}_0 + o(1)$ and $\hat{b} = \hat{b}_0 + \mu\hat{b}_1 + \nu\tilde{b} + o(\mu)$. Substituting the expansion above into (10b), we find the same leading order solution as in section 2.2. Explicitly

$$\hat{S}_0 = \hat{h}^{-1}(b_c - b_0), \qquad \hat{u}_0 = \frac{q}{\hat{S}_0}$$

where $b_c = b_0(x_c(t), t)$ is the seal height at the downstream end of the ponded section. At first order, defining $\hat{h}_1 = h'(\hat{S}_0)\hat{S}_1$

$$\begin{aligned}\hat{h}_{1,x} =& -\hat{b}_{1,x} - \frac{q^2}{\hat{S}_0^3}\hat{P}\left(\hat{S}_0\right) + \frac{Fr^2 h^{-1}(\nu^{-1})}{P(h^{-1}(\nu^{-1}))}\frac{q^2\hat{S}_{0,x}}{\hat{S}_0^3} \\ =& -\hat{b}_{1,x} - \frac{q^2}{\hat{S}_0^3}\hat{P}\left(\hat{S}_0\right) - \frac{Fr^2 h^{-1}(\nu^{-1})}{P(h^{-1}(\nu^{-1}))}\frac{q^2 b_{0,x}}{\hat{h}'(\hat{S}_0)\hat{S}_0^3}, \qquad (31)\end{aligned}$$

$$b_{1,t} + Ub_{1,x} = \frac{1}{P(h^{-1}(\nu^{-1}))}\frac{q^3}{\hat{S}_0^3}, \qquad (32)$$

and water level $h_w = \hat{h}(\hat{S}) + b = h_{w0} + \nu\tilde{h}_w + \mu h_{w1}$ to first order satisfies

$$h_{w0,x} = 0, \qquad \tilde{h}_{w,x} = 0, \qquad h_{w1,x} = \hat{h}_{1,x} + b_{1,x} = -\frac{q^2}{\hat{S}_0^3}\hat{P}\left(\hat{S}_0\right) - \frac{Fr^2 h^{-1}(\nu^{-1})}{P(h^{-1}(\nu^{-1}))}\frac{q^2 b_{0,x}}{\hat{h}'(\hat{S}_0)\hat{S}_0^3}. \tag{33}$$

At issue is the behaviour of $h_{w,1}$ and b_1 near the end points of a ponded section, where $\hat{S}_0 \to 0$ and hence the slope of the correction terms $\hat{h}_{1,x}$ and $\hat{b}_{1,x}$ diverge. Note that the limiting forms as $x \to x_c$ of the right-hand sides of (32) and of (33) correspond to rescaled versions of the limiting behaviour as $X \to -\infty$ of $B_X - b_{0x}^-$ and $H_{w,X}$ and in (25) and (28), where $\hat{h}'$ and h' have matching limiting forms as $\hat{S} \to 0$, $\Sigma \to \infty$, ensuring that the solutions can be matched, with a bounded composite solution (Holmes, 1995).

Specifically, note that h_{w1} can be solved by quadrature since $\hat{S}_0$ is known. Key to the behaviour of h_{w1} is whether the right-hand side of $(33)_3$ is integrable up to $x = x_c$. As in the boundary layer, we can switch to $\hat{S}_0$ as the variable of integration using $\partial\hat{S}_0/\partial x = -b_{0x}/h'(\hat{S}_0)$, recognizing that $\hat{S}_0 \to 0$ as $x \to x_c$. When doing so, we obtain an integral of the form

$$\int \frac{q^2\hat{P}(\hat{S}_0)\hat{h}'(\hat{S}_0)}{b_{0x}\hat{S}_0^3} + \frac{Fr^2 h^{-1}(\nu^{-1})}{P(h^{-1}(\nu^{-1}))}\frac{q^2}{\hat{S}_0^3}\mathrm{d}\hat{S}_0 \tag{34}$$

These again take the same limiting form (when $b_{0x} \to b_{0x}^-$) as the integrands in (29)–(30), only that our concern is now with taking the limit of integration to zero rather than infinity. Clearly, $q^2/\hat{S}_0$ is not integrable down to $\hat{S}_0$, but the corresponding inner integral in (29) converges as $\Sigma \to \infty$.

The first term in the integrand in (34) is harder to deal with. Consider first the case where P and h, and therefore their rescaled versions $\hat{P}$ and $\hat{h}$ are simple power laws or exponential functions. Ignoring the marginal case in which the integral of $q^2P(\Sigma)h'(\Sigma)/\Sigma^3$ diverges $\Sigma \to \infty$ *and* the integral of $q^3\hat{P}(\hat{S}_0)h'(\hat{S}_0)/\hat{S}_0^3$ diverges as $\hat{S}_0 \to 0$ (which would be the case if both integrands behave as $1/\Sigma$, or $1/\hat{S}_0$ for both large and small Σ and $\hat{S}_0$), then we conclude that either the integral over $H_{w,X}$ converges as $X \to -\infty$ or the integral over $h_{w1,x}$ converges as $x \to x_c$.

For the former case, which as discussed includes the power laws considered in the main paper, $\tilde{h}_w = H_w(-\infty, T)$ and h_{w1} is unbounded as $x \to x_c$, but a bounded composite solution can be constructed as

$$h_w(t) = b(x_c(t), t) + \nu H_w(\nu^{-1}(x - x_c(t)), t) + \mu\breve{h}_{w,1} + o(\nu) + o(\mu) \tag{35}$$

where $\breve{h}_{w,1}$ satisfies

$$\begin{aligned}\breve{h}_{w1,x} =& h_{w1,x} + \frac{q^2\hat{P}(h^{-1}(b_{0x}^-(x_c(t) - x))}{[h^{-1}(b_{0x}^-(x_c(t) - x))]^3} \\ &+ \frac{Fr^2 h^{-1}(\nu^{-1})}{P(h^{-1}(\nu^{-1}))}\frac{q^2 b_{0x}^-}{\hat{h}'(h^{-1}(b_{0x}^-(x_c(t) - x)))[h^{-1}(b_{0x}^-(x_c(t) - x))]^3}\end{aligned} \tag{36}$$

For the latter case, in which $\hat{P}(\hat{S}_0)/\hat{S}_0^3$ is integrable to $\hat{S}_0 = 0$, neither H_w nor h_{w1} are bounded, and a slightly more elaborate composite solution is possible, of the form

$$h_w(t) = b(x_c(t), t) + \nu\breve{H}_w((x - x_c(t))/\nu, t) + \mu\breve{h}_{w,1}(x, t) + o(\nu) + o(\mu) \tag{37}$$

where

$$\breve{H}_{w,X} = H_{w,X} + \frac{q^2 P(h^{-1}(-b_{0x}^- X))}{h^{-1}(-b_{0x}^- X)}, \tag{38a}$$

$$\breve{h}_{w,x} = h_{w1,x} + \frac{Fr^2 h^{-1}(\nu^{-1})}{P(h^{-1}(\nu^{-1}))}\frac{q^2 b_{0x}^-}{\hat{h}'(h^{-1}(b_{0x}^-(x_c(t) - x)))[h^{-1}(b_{0x}^-(x_c(t) - x))]^3} \tag{38b}$$

By construction, $\breve{H}_w$ and $\breve{h}_w$ remain bounded, since the unbounded limiting behaviour in H_w is accounted for the corresponding limiting behaviour in h_w and vice versa. In both cases, the composite solution takes the form $h_w = b(x_c(t), t) + O(\nu) + O(\mu)$, confirming the leading order solution for the ponded region in section 2.2.

If P and h are more complicated, for instance of the form $h(\Sigma) = c_1\Sigma^{\beta_1} + c_2\Sigma^{\beta_2}$, then the definition of $\hat{h}$ and $\hat{P}$ in (11) may lead to neither $P(\Sigma)h'(\Sigma)/\Sigma^3$ being integrable as $\Sigma \to \infty$, not $\hat{P}(\hat{S}_0)\hat{h}'(\hat{S}_0)/\hat{S}_0^3$ being integrable as $\hat{S}_0 \to 0$. However, in that case, $\hat{h}$ or $\hat{P}$ as defined in through (11) will contain terms that are of higher order, and need to be accounted for by expanding $\hat{h}$ and $\hat{P}$, as well as expanding $\hat{S}$ to higher than first order in μ. This is unfeasible to illustrate here bar for concrete cases: a bounded composite solution remains possible in the standard way, by absorbing non-integrable terms in $H_{w,X}$ in the appropriate order of expansion in h_w and vice versa, as in (38).

B and b_1 can be dealt with in much the same way, except that b_1 is slightly more complicated to solve for using characteristics. If $h'(\Sigma)/\Sigma^3$ is integrable as $\Sigma \to \infty$ and B is therefore bounded, while $\hat{h}'(\hat{S}_0)/\hat{S}_03$ is not integrable as $\hat{S}_0 \to 0$, then $\tilde{b} = B(-\infty, T)$ and the appropriate composite solution is

$$b(x,t) = b_0(x,t) - b_{0x}^-(x - x_c(t)) + \nu B((x - x_c(t))/\nu, t) + \mu\breve{b}_1(x,t) \tag{39}$$

where $\breve{b}(x,t)$ satisfies

$$\breve{b}_{1,t} + U\breve{b}_{1,x} = \frac{1}{P(h^{-1}(\nu^{-1}))}\left[\frac{q^3}{\hat{S}_0^3} - \frac{q^3}{[h^{-1}(b_{0x}(x_c(t) - x))]^3}\right] \tag{40}$$

whereas for the opposite case in which $\hat{h}'(\hat{S}_0)/\hat{S}_03$ is bounded as $\hat{S}_0 \to 0$ while $h'(\Sigma)/\Sigma^3$ is not integrable as $\Sigma \to \infty$, the composite solution takes the form

$$b(x,t) = b_0(x,t) - b_{0x}^-(x - x_c(t)) + \mu b_1(x,t) + \breve{B}((x - x_c(t))/\nu, t) \tag{41}$$

where $\breve{B}$ satisfies

$$\breve{B}_X = B_X - \frac{q^3}{(U - \dot{x}_c)[h^{-1}(-b_{0x}^- X)]^3} \tag{42}$$

2.7 Upstream end of a ponded section

A flowing section entering a ponded section can be treated using (17), since only matching with the downsteam far field is at issue. If that far field is ponded, we abandon the relationship $V_\infty^2 P(qV_\infty^{-1}) = -qV_\infty^{-1}b_{0x}^+$ and simply put $V_\infty = 0$. Assuming that P is concave as before, a solution such that $V \to -V_\infty$ as $X \to -\infty$ and $V \to 0$ as $X \to \infty$ requires that $V_{-\infty}$ be unstable, which is the case if and only if

$$\frac{3V_{-\infty}^2 P\left(\frac{q}{V_{-\infty}}\right)}{q} - V_{-\infty}P'\left(\frac{q}{V_{-\infty}}\right) - \frac{3V_{-\infty}^2}{U - \dot{x}_c} \geq 0. \tag{43}$$

We still assume that P is concave and hence that $S/P(S)$ is a non-decreasing function of S. By the same argument as that following (17), it follows that if $V_{-\infty}$ is an unstable fixed point, then there is a solution connection $V_{-\infty}$ to $V = 0$: (17) can have two fixed points (0 and $V_{-\infty}$) or three (0, V_∞ and a second root V_∞ of the second square brackets in (17)). The existence of the desired solution is only in question in the latter case. However, the argument following (17) shows that if $V_{-\infty}$ is stable, it is the smaller of the two roots, and the desired solution therefore exists.

With P being cancave, $P'(S) \leq P(S)/S$ and the sum of the first two terms in (43) is positive. Hence (43) is satisfied if

$$\dot{x}_c > U \tag{44}$$

or if

$$\dot{x}_c \leq U - \frac{3qV_{-\infty}^2}{3V_{-\infty}^2 P\left(\frac{q}{V_{-\infty}}\right) - qV_{-\infty}P'\left(\frac{q}{V_{-\infty}}\right)}. \tag{45}$$

The slope derivative M_{-p} of the melt rate M is defined through (5) and (8). With $V_{-\infty}$ defined through $V_{-\infty}^2 P(q/V_{-\infty}) = qV_{infty}^{-1} b_{0x}^-$, (45) becomes

$$\dot{x}_c < U - M_{-p}(-b_{x0}^-, q). \tag{46}$$

As in appendices B3 and C of the main paper, (44) and (46) together state that the transition point x_c must either travel at the same speed or more slowly than characteristics entering the transition from the left (if (46) holds), or travel faster than characteristics entering the transition from the right (if (44) holds). We also still obtain a relationship between the jump in slope and migration rate, since

$$B_X = b_{0x}^- + \frac{V_{-\infty}^3 - V^3}{U - \dot{x}_c} \to b_{0x}^- + \frac{V_{-\infty}^3}{U - \dot{x}_c} \tag{47}$$

as $X \to \infty$, so $b_{0x}^+ - b_{0x}^- = M(b_{0x}^-, q)/(U - \dot{x}_c)$. These results again mirror those in the main paper.

2.8 A smooth seal

The boundary layer description in appendix 2.5 assumes the seal to correspond to a shock with $b_{0x}^- > 0$ and $b_{0x}^+ < 0$. This excludes the possibility of a smooth seal in the outer problem as explored in the main paper. Here we revisit the boundary layer problem, assuming such a smooth seal. For simplicity, we restrict ourselves to the simple consitutive relations of the main paper, $P(S) = S^\alpha$ and $h(S) = S^\beta$.

In that case an alternative rescaling takes the place of (14)

$$\tilde{B} = \frac{b(x,t) - b_0(x_s(t),t)}{\nu^{(6-2\alpha)/(6-2\alpha+\beta)}}, \qquad \tilde{V} = \frac{u}{\nu^{1/(6-2\alpha+\beta)}}, \qquad \tilde{\Sigma} = \nu^{1/(6-2\alpha+\beta)} S, \qquad \tilde{X} = \frac{x - x_s(t)}{\nu^{(3-\alpha)/(6-2\alpha+\beta)}},$$

and we assume that $b_{0x}(x_s(t),t) = 0$. At leading order, the rescaled model becomes

$$(\tilde{\Sigma}\tilde{V})_{\tilde{X}} = 0, \qquad -\tilde{V}^2\tilde{\Sigma}^\alpha - \tilde{\Sigma}\tilde{B}_{\tilde{X}} - \beta\tilde{\Sigma}^\beta\tilde{\Sigma}_{\tilde{X}} = 0, \qquad b_{0,t}(x_s(t),t) = w(x_s(t)). \tag{48}$$

Expanding to first order, we additionally obtain

$$(U - \dot{x}_s)\tilde{B}_{\tilde{X}} = w_x(x_s(t))\tilde{X} - I_\alpha \tilde{V}^3, \tag{49}$$

where $I_\alpha = 1$ if $\alpha = 0$, $I_\alpha = 0$ otherwise. The boundary layer model can be rewritten as a modified version of (22b)

$$\tilde{V}_{\tilde{X}} = \frac{\tilde{V}^{1+\beta}}{\beta q^\beta}\left(\frac{\tilde{V}^{3-\alpha}}{q^{1-\alpha}} + \frac{w_x}{U - \dot{x}_s}\tilde{X} - I_\alpha \frac{\tilde{V}^3}{U - \dot{x}_s}\right). \tag{50}$$

We need to match $\tilde{V} \to 0$ as $\tilde{X} \to -\infty$ and $V \sim [-q^{1-\alpha}w_x\tilde{X}/(U - \dot{x}_s - I_\alpha q^{1-\alpha})]^{1/(3-\alpha)}$ as $\tilde{X} \to \infty$. We can analyze the limiting behaviour of V by transforming (away from $\tilde{X} = 0$) independent and dependent variables to $\Psi = |\tilde{X}|^{-1/(3-\alpha)}\tilde{V}$ and $\zeta = (3-\alpha)/(6-2\alpha+\beta)\,\mathrm{sgn}(\tilde{X})|\tilde{X}|^{(3-\alpha)(6-2\alpha+\beta)}$, and introducing an auxiliary variable $\phi = |\zeta|^{-1/2}$. We can then rewrite (50) as an effectively autonomous system

$$\Psi_\zeta = -\frac{\mathrm{sgn}(\zeta)\phi^2\Psi}{6-2\alpha-\beta} + \frac{\Psi^{1+\beta}}{\beta q^\beta}\left[\frac{\Psi^{3-\alpha}}{q^{1-\alpha}} - I_\alpha\frac{\Psi^3}{U-\dot{x}_s} + \frac{\mathrm{sgn}(\zeta)w_x}{U-\dot{x}_s}\right], \qquad \phi_\zeta = -\,\mathrm{sgn}(\zeta)\phi^3, \tag{51}$$

where the trajectory chosen must satisfy $\phi = |\zeta|^{-1/2}$ as stated, and the matching conditions dictate that $\Psi \to 0$ as $\zeta \to -\infty$, $\Psi \to \Psi_\infty = [-qw_x/(U - \dot{x}_s - I_\alpha q^{1-\alpha})]^{1/(3-\alpha)}$ as $\zeta \to \infty$. Ψ (like $\tilde{V}$) must be positive. The outer solution dictates that $U - \dot{x}_s = w_x/b^-_{0xx}$ is of the opposite sign to w_x. This ensures that a fixed point with positive Ψ exists if $\alpha > 0$. For $\alpha = 0$, existence of such a fixed point is conditional: if $w_x < 0$, we must have $U - \dot{x}_s > q > 0$ or $w_x > 0$, $U - \dot{x}_s < 0 < q$. These statements are the same as the corresponding constraints on smooth seals in the main paper.

With $w_x/(U - \dot{x}_s) < 0$, we further find that $(\Psi, \phi) = (\Psi_\infty, 0)$ is a degenerate saddle with a unique orbit (the centre manifold) into the fixed point, while the fixed point $(\Psi, \phi) = (0, 0)$ is a degenerate unstable node, with all nearby orbits converging to the origin as $\zeta \to -\infty$. These conditions allow a unique solution of the original problem (50) that satisfies both matching conditions. Using the same approach as sketched in the previous section, we can also again demonstrate that water level in the upstream far field exceeds seal height by an amount of $O(\nu^{(6-2\alpha)/(6-2\alpha+\beta)}) \ll 1$, again justifying the derivation of the ponding function in section 2.2.

3 Supercritical flow

3.1 Hydraulic jump in a lake seal

A key restriction in our boundary layer models in section 2.3 is that the flow must remain subcritical, with $qh'(q/V) > Fr^2V^3$. Consider for example the seal boundary layer of section 2.5, so (22) holds. Now consider V crossing criticality at V_c defined implicitly through $qh'(q/V) > Fr^2V^3$. In order to go through criticality at finite X, we have to prevent a the right-hand side from becoming singular, so

$$b^-_{0x} + \frac{V_c^{3-\alpha}}{q^{1-\alpha}} - \frac{V_c^3}{U - \dot{x}_c} = 0$$

and we can compute the migration rate of the seal purely in terms of the slope b^-_{0x} of the channel base upstream of the the seal, and through V_c, in terms of the Froude number Fr and the water flux q:

$$\dot{x}_c = U - \frac{q^{1-\alpha}V_c^3}{q^{1-\alpha}b^-_{0x} + V_c^{3-\alpha}}. \tag{52}$$

So long as we are assured that a hydraulic jump from sub- to supercritical occurs in the seal, we appear to have a simpler model for seal evolution, in the sense that it does not require us to solve (3) downstream. This is analogous to the supercritical case in Kingslake and others (2015).

This last result may however be misleading. As we show immediately below, supercritical flow does not allow the downstream far field to satisfy (2), since recurring structures at the short $O(\nu)$ length scales are bound to emerge, and the boundary layer construction no longer applies: the matching procedure with the downstream solution does not apply when the latter is unstable. In addition, in the absence of a viable outer model on the downstream side of the 'shock', (52), we have no information on how that downstream side evolves and therefore whether the shock will continue to represent a transition to supercritical flow (which in itself presumably depends on how steep the downstream slope b^+_x is).

3.2 Roll waves and bedforms

We sketch the instabilities leading to that structure only very briefly here, since it is closely related to known features of the St Venant equations (Fowler, 2011, sections 4.4.4–4.5.2 and chapter 5).

Instabilities occur at the same short $O(\nu)$ length scale as the boundary layers, and we use a local coordinate system travelling at the ice velocity U, putting $\xi = \nu^{-1}(x - Ut)$, $\tau = t$ and $B = \nu^{-1}b$. The scaled model (1) becomes

$$\begin{aligned} \delta\nu S_\tau + [(u - \delta U)S]_\xi &= \varepsilon\nu u^3 P(S)\alpha \\ Fr^2 S[\delta\nu u_\tau + (u - \delta U)u_\xi] &= -u^2 P(S) - SB_\xi - Sh(S)_\xi \\ B_\tau &= w - u^3 \end{aligned}$$

We drop terms of $O(\delta)$, $O(\nu)$ and $O(\varepsilon)$ again, except for the time derivatives S_τ and u_τ, which represent singular perturbations that are in fact indicative of fast time scale dynamics.

Consider a constant uplift rate $w > 0$, and a steady state solution of (1) with all terms but the $O(\varepsilon)$ melt term retained. Denoting the steady state by overbars, we have $\bar{B}(\xi) = \bar{B}_\xi \xi$, $\bar{u} = w^{1/3}$ and $\bar{S}/P(\bar{S}) = -\bar{u}^2/\bar{B}_\xi$. Perturbing the steady state as $B = \bar{B} + B' \exp(ik\xi + \sigma\tau)$, $u = \bar{u} + u' \exp(ik\xi + \sigma\tau)$, $S = \bar{S} + S' \exp(ik\xi + \sigma\tau)$, we obtain

$$\begin{aligned} (\delta\nu\sigma + ik\bar{u})S' + ik\bar{S}u' &= 0 \\ Fr^2\bar{S}(\delta\nu\sigma + ik\bar{u})u' &= -2\bar{u}P(\bar{S})u' - \bar{u}^2 P'(\bar{S})S' - ik\bar{S}B' - \bar{B}_\xi S' - ik\bar{S}h'(\bar{S})S' \\ \sigma B' &= -3\bar{u}^2 u' \end{aligned}$$

There are three roots, and in the limit of $\delta\nu \ll 1$, we can look separately at roots $\sigma \sim O(1)$ and $O(\delta^{-1}\nu^{-1})$ separately. For the latter, we have at leading order that $B' = 0$ and

$$\sigma \sim \frac{1}{\delta\nu}\left[-[ik\bar{u} + Fr^{-2}\bar{u}P(\bar{S})/\bar{S}] \pm \sqrt{Fr^{-4}\bar{u}^2 P(\bar{S})^2/\bar{S}^2 - ikFr^{-2}\bar{u}^2[P(\bar{S})/\bar{S} - P'(\bar{S})] - k^2 Fr^{-2}\bar{S}h'(\bar{S})}\right]$$

This is the dispersion relation for the St Venant equations studied in Fowler (2011, sections 4.4.4 and 4.5), and has roots with a positive real part when $Fr^2\bar{u}^2/\bar{S}h'(\bar{S})) > 4[1 - \bar{S}P'(\bar{S})/P(\bar{S})]^{-2}$, with instability leading to roll wave formation. When that instability criterion is satisfied, we find non-vanishing growth rate $\Re(\sigma)$. in the limit $k \to 0$ as discussed in Fowler (2011): a turbulent extensional stress term added to the model may suppress growth of short wavelengths, but given the hyperbolic nature of the roll wave problem, it is not clear *a priori* that a lack of suppression of short wavelengths renders the model ill-posed.

For the $O(1)$ root, we have

$$\sigma \sim \frac{3ik\bar{u}^3}{[P(\bar{S}/\bar{S} - P'(\bar{S})]\bar{u}^2 + ik(Fr^2\bar{u}^2 - \bar{S}h'(\bar{S})}$$

and we have $B' \neq 0$; this solution describes bedform formation with $\Re(\sigma) > 0$ when the flow is supercritical with $Fr^2\bar{u}^2 > \bar{S}h'(\bar{S})$ or $Fr^2\bar{u}^3/[qh'(q/\bar{u})] >$. This is the same criterion as for supercriticality in the boundary layer solutions of sections 2.3 above. As $4[1 - \bar{S}P'(\bar{S})/P(\bar{S})]^{-2} > 1$, bedforms are predicted at lower velocities than roll waves. We expect to see bedform formation at lower flow speeds than we see roll waves. We still have a short wave instabilities with $\Re(\sigma) \sim 3\bar{u}^3/(Fr^2\bar{u}^2 - \beta\bar{S}^\beta)$ as $k \to \infty$, and a stabilizing mechanism may again be needed: a more sophisticated heat transfer model is a likely candidate, in which dissipation does not instantly cause melting, and heat can be advected. As advection becomes dominant at short wavelengths, we may expect to suppress short wavelength growth.

The formation of short-wavelength structure at supercritical Froude numbers shows that the model (2) must be modified. Unlike in section 2.3, that structure is not localized. Instead of a boundary layer approach, incorporation into a large-scale model analogous to (2) therefore requires a multiple scales approach (Holmes, 1995), which represents a promising avenue for future research.

4 Breaching the seal

Here we revisit the question of a critical steady water input Q to the lake at which the lake seal must be breached eventually. In the main paper, we identified such a critical water input by determining when a steady state solution fails to exist. Here, we argue that failure of a steady state to exist implies that upward-migrating shocks will form and breach the seal.

4.1 Preliminaries: restatement of the problem and key results

First, the leading order model in question, which consists of (3)–(4) combined with the lake mass balance model

$$b_m = \sup_{x>0} b(x,t) \tag{53a}$$

$$\gamma \dot{h}_0 = Q(t) - q, \tag{53b}$$

$$q = \begin{cases} 0 & \text{if } h_0 < b_m, \\ \max\left(Q - \gamma \dot{b}_m, 0\right) & \text{if } h_0 = b_m, \end{cases} \tag{53c}$$

where we denote the seal location by $x_m(t)$, with $b(x_m(t),t) = b_m(t)$.

The argument below will make use of a results that are derived in the main paper. First, (3) can be treated as being of Hamilton-Jacobi form

$$b_t = -\mathcal{H}(x,t,p,q)$$

if $\mathcal{H}(x,t,p,q) = Up - c(x,t)M(-p,q)$, and x, b and $p = b_x$ satisfy the following evolution equations in terms of characteristic variables (σ,τ),

$$x_\tau = \mathcal{H}_p, \qquad b_\tau = -\mathcal{H} + \mathcal{H}_p p, \qquad p_\tau = -\mathcal{H}_x, \qquad t_\tau = 1.$$

Given these, we can define $\tilde{\mathcal{H}}(\sigma,\tau) = \mathcal{H}(x(\sigma,\tau),\tau.p(\sigma,\tau),q(\tau))$ as the Hamiltonian defined as a function of the characteristic variables. Along a characteristic then we have

$$\tilde{\mathcal{H}}_\tau = \mathcal{H}_x x_\tau + \mathcal{H}_p p_\tau + \mathcal{H}_q q_\tau = \mathcal{H}_q q_\tau, \tag{54}$$

assuming that the characteristic in question does not enter into a ponded section from above: for a characteristic entering into a ponded section cM will generally be discontinuous at the transition from flowing to ponded: in fact, appendix C of the main paper can be used to show $\tilde{H}$ jumps on entry into a pond unless the upstream end x_p of the ponded section is steady in time. If a characteristic does not enter into a ponded section from above and q is constant, then $\tilde{\mathcal{H}}$ therefore remains constant. When q does change, q_τ may need to be treated as a delta distribution as appropriate.

As upstream boundary condition on (3) we impose $b(0,t) = b_{in}(0) =$ constant, and hence we must have $\mathcal{H} = 0$ at $x = 0$. Upstream of the lake seal, $c = 0$ and hence $\mathcal{H}_q = 0$. Any characteristic that originates at the upstream end of the domain therefore has $\tilde{\mathcal{H}} = 0$, and the downstream propagation of such characteristics will rapidly establish a locally steady solution unless there is an upstream-migrating shock. Barring such a shock, a steady seal will form.

Below, we will be concerned with seals, either at the downstream end of the lake, or at the end of a ponded section. If a seal at $x = x_s$ is 'smooth' with $b_x(x_s,t)^- = 0$, then

$$\dot{x}_s = U - \frac{w_x(x_s)}{b^-_{xx}(x_s,t)} = U - M_{-p}(0^-,q) - \frac{w_x(x_s)}{b^+_{xx}(x_s,t)}. \tag{55}$$

where superscripts + and − denote limits taken as x_s is approached from above and below, respectively, and M_{-p} denotes the derivative of $M(-p,q)$ with respect to its first argument.

Seal height for a smooth seal $b_s(t) = b(x_s(t),t)$ evolves as

$$\dot{b}_s = b_t^- + \dot{x}_s b_x^- = w(x_s), \tag{56}$$

so a steady smooth seal is located where $w(x_s) = 0$. Consider in particular the lake seal at $x_s = x_m$ and suppose that this seal is both 'smooth' and steady, so $Ub_x(\bar{x}_m) = w(\bar{x}_m) = 0$. Maintaining the smooth seal in steady state requires characteristics to the right of the seal to travel downstream, with

$$x_\tau = U - M_{-p}(0^-,q) > 0. \tag{57}$$

If instead of a smooth seal, there is a shock, the location x_s and height b_s of that shock (whether at the end of the lake of a downstream ponded section) evolve as

$$\dot{x}_s = \frac{\mathcal{H}^+ - \mathcal{H}^-}{b_x^+ - b_x^-} = U + \frac{M(-b_x^+,q)}{b_x^+ - b_x^-}, \qquad \dot{b}_s = b_t + b_x\dot{x}_s = w(x_m) + \frac{b_x^- M(-b_x^+,q)}{b_x^+ - b_x^-} \tag{58}$$

If, as we will assume, the lake is full with $h_0 = b_m$, then $Q = q$ while the seal is in steady state. By contrast, if a steady state seal, with b in steady state upstream of the seal, is 'breached' with $\dot{x}_s < 0$, it is clear that

$$\dot{b}_m = b_t + b_x^-\dot{x}_s = b_x^-\dot{x}_s \le 0 \tag{59}$$

since $b_t = 0$ and $b_x^- \ge 0$ immediately upstream of the seal. Consequently, once the seal is breached, q increases by (53). By (54), $\tilde{\mathcal{H}}$ then increases for any characteristic in a flowing section, where $\mathcal{H}_q > 0$, while remaining constant for any characteristic in a ponded section, including upstream of the seal.

Below, we will also need to consider characteristics that travel upstream from a ponded section towards the lake seal. Unless the upstream end $x_p(t)$ of the section migrates downstream at velocities greater than U (a circumstance we will be able to discount) such upward-propagating characteristics emerge from an expansion fan, If the water level in the pond (itself set by the seal at the downstream end of the pond) is denoted by $b(x_p(t),t) = b_p$, then appendix C of the main paper shows that characteristics in the expansion fan emerge at slopes $p^- = b_x^-$ such that

$$\dot{b}_p = -\mathcal{H}^- + p^-\mathcal{H}_p^- = b_\tau^-, \tag{60}$$

where $\mathcal{H}^-$ is the Hamiltonian evaluated at $x = x_p(t)$ and $p = p^-$.

4.2 Breaching of the seal by upward-propagating characteristics

Next, we consider the conditions for breaching of a steady seal as advertised. As in the main paper, we assume that $w(x)$ has a single zero at $x = \bar{x}_m$ and $w(x) < 0$ for $x > \bar{x}_m$, and that $b(x)$ is initially in steady-state upstream of the seal, with $Ub_{in.x} = w > 0$ for $x < \bar{x}_m$. Our main interest is in how the seal is breached, that is, in how a backward-migrating shock can form at the lake seal $x = \bar{x}_m$, or migrate up to the seal. By (54), the value of the Hamiltonian $\tilde{\mathcal{H}}$ on any given characteristic is constant prior to seal incision, and $\tilde{\mathcal{H}}$ increases immediately after seal incision (when $q_\tau > 0$) on characteristics below the seal, while $\tilde{\mathcal{H}}$ remains constant on characteristics above the seal.

Consider first $\alpha = 0$, for which $M(-p,q) = H(-p)pq$. Here, the main paper shows that steady states are impossible if $Q > U$. As described in the main paper, we require $Q < U$ for a steady-state solution in which $q = Q$, $b_{xx}^- = Uw_x$ and $M_{-p}(0^-,q) = Q$. When instead $Q > U$, characteristics

downstream of the seal initially propagate upstream at velocity $x_\tau = U - M_{-p}(-p,q) = U - Q$, while characteristics upstream of the seal travel at $x_\tau = U$. By (54), the characteristics that arrive at the nascent shock from upstream have $\tilde{H} = 0$, while those arriving from downstream have $\tilde{\mathcal{H}} > 0$ if initial conditions are such that $\tilde{\mathcal{H}}(\sigma, 0) > 0$ downstream of the seal. The latter is certainly the case if the initial profile $b_{in} = s$ is at the unincised ice surface, with $Ub_{in,x} = w$ along the entire domain as in the solutions computed numerically in the main paper. In that case, $\tilde{H} = cM(-b_{in,x}, Q) > 0$ downstream of the seal. In that case, we have $\mathcal{H}^+ > 0$, $\mathcal{H}^- = 0$ and $b_x^+ < 0 < b_x^-$ for the nascent shock, which therefore migrates upstream by equation (58).

Consider next the more complicated case of $\alpha > 0$. Here, the reduced Hamiltonian $\mathcal{H}_r(p,q) = Up + M(-p,q)$ has a global minimum $\mathcal{H}_c(q)$ in the absence of ponding, and a steady state is impossible if $\inf(w) < \mathcal{H}_c(Q)$. In fact, we can then identify a part of the domain in which $\mathcal{H} = \mathcal{H}_r - w > 0$ in the absence of ponding. We call this part of the domain the 'barrier' since no characteristic on which $\tilde{\mathcal{H}} \leq 0$ can pass through the barrier. We argue below that the presence of this barrier ultimately causes characteristics with $\tilde{\mathcal{H}} > 0$ to travel upstream from the barrier and form shocks that continue migrating upstream until the seal of the lake is breached.

Assume first that there is indeed no ponding below the seal. If characteristics that start between seal and barrier do not propagate upstream and breach the seal, then eventually characteristics with $\tilde{\mathcal{H}} > 0$ will emerge from the upstream end of the barrier and propagate upstream to a shock that is bound to migrate upstream until it breaches the seal. This occurs at the latest when characteristics that originate above the seal with $\tilde{\mathcal{H}} = 0$ reach the upstream end of the barrier. It is easy to see that, if this happens, then these characteristics are bound to reverse direction, since they cannot propagate into the barrier. With $w_x < 0$ at the upstream end of the barrier, p decreases with τ there, forcing p on these characteristics to pass the critical value $p_c(Q)$, causing the reversal of direction. By continuity or through the formation of an expansion fan, characteristics must then also emerge from the barrier itself, with $\tilde{\mathcal{H}} > 0$ by construction of the barrier. It is easy to show that these characteristics cannot change direction between seal and barrier since $w > \mathcal{H}_c(Q)$ and hence, with $\mathcal{H}_r = \mathcal{H} + w > \mathcal{H}_c(Q)$, p cannot pass through the critical slope $p_c(Q)$ at which characteristics change direction. If these characteristics encounter a shock where they collide with characteristics that originate upstream of the seal, the shock is bound to migrate upsteam by $(58)_1$, eventually reaching the seal itself.

The argument above needs modification if the barrier becomes ponded. Since we necessarily have $b_t = -\mathcal{H} < 0$ in the barrier, ponding in the barrier region is a real possibility as shown in figures 7–8 of the main paper. With $w < 0$ downstream of the steady lake seal at $\bar{x}_m$, any ponded section with its own seal height b_p downstream of $\bar{x}_m$ is guaranteed to have $\dot{b}_p < 0$ by $(58)_2$ and (56). Suppose then that such a ponded section forms around the barrier, and denote the upstream end of that ponded section by x_p.

We can discount x_p migrating downstream, since that would move the ponded section below the barrier and the previous situation would apply once more. Suppose therefore that $\dot{x}_p \leq 0$. By appendix C of the main paper, there are then two possibilities: either characteristics enter x_p from above, or an expansion fan forms and new characteristics are generated tangentially to $x_p(t)$. The former case cannot persist indefinitely: characteristics entering x_p from above would eventually be those originating upstream of the seal, implying a local steady state. That is however at odds with the fact that $\dot{b}_p < 0$. If therefore characteristics emerge from the upstream end of the ponded area, with $\dot{x}_p \leq 0$, then (60) with $\dot{b}_p < 0$ and with $x_\tau = \mathcal{H}_p \leq 0$ (since the characteristics are propagating upstream or stationary has $\tilde{\mathcal{H}} > 0$ on those characteristics. As with the upstream end of the barrier, backward-propagating characteristics with $\tilde{\mathcal{H}}$ are predicted to form at the upstream end of the ponded region, and will again lead to the formation of a backward-migrating shock that

breaches the seal.

Note that in both cases, we have argued that the shock that forms at the seal or reaches the seal will continue to migrate backwards. In general, this only true at the instant at which the shock passes the seal, since we know that q is non-decreasing at that point, and therefore the Hamiltonian $\tilde{\mathcal{H}}$ on characteristics reaching the shock from downstream is positive by (54). This need not be the case indefinitely, since the flux q need not continue to increase beyond the initial seal incision: the evolution of flux q over time us governed by $q = \max(Q - \gamma \dot{b}_m)$ where

$$\dot{b}_m = b_t^- + b_x^- \frac{\mathcal{H}^+ - \mathcal{H}^-}{b_x^+ - b_x^-} = b_x^- \frac{\mathcal{H}^+}{b_x^+ - b_x^-}$$

for the geometry assumed here. It is apparent that $\dot{b}_m$ may decrease with time even if the shock continues to propagate upstream: this is true especially if the slope b_x^- upstream of the seal decreases during incision. If q then decreases over time, so will $\tilde{\mathcal{H}}$ on characteristics reaching the shock from above, which may eventually lead to the shock ceasing its upward migration, as is evident in some of the numerical solution: lake drainage can spontaneously cease without the lake having been emptied completely. It is worth noting however that, if $\gamma = 0$, then $q = Q$ while the lake is being drained, and with $q_\tau = 0$, $\tilde{\mathcal{H}}$ on characteristics reaching the seal-breaching shock from downstream will remain positive, ensuring the seal continues to migrate upstream. This is consistent with the numerical results in the main paper, where spontaneous halting of lake drainage is associated with larger values of γ and the slope b_x flattening upstream of the steady state seal location, as well as with $\alpha > 0$.

5 Numerical calculations

5.1 The case $\alpha = 0$

The main paper only provided a brief description of results for the not strictly convex case $\alpha = 0$, for which shock formation and the relationship between flux q and near-seal geometry are qualitatively different from the strictly convex case. Here we provide a more detailed overview in the form of figure 2, where we use the unregularized version of the model, allowing for blow-up of the solution for q as discussed in the main paper. As pointed out in the main paper, there are no oscillatory solutions for $\alpha = 0$ in figure 2

Once the seal is breached, the outcome of lake drainage depends on both Q and γ. As already indicated above, for $\alpha = 0.5$, moderate Q and larger γ favour oscillatory drainage of the lake, with smaller Q and larger γ ultimately also leading to periodic oscillations rather than divergent oscillations eventually leading to lake drainage. For $\alpha = 0$, ; oscillatory lake drainage does not occur in any of the computations we have performed.

For $\alpha = 0$, smaller Q and larger γ by contrast favour blow-up of the solution with singular outflow q. Oscillatory lake drainage does not occur in any of the computations we have performed. Recall that oscillatory behaviour for $\alpha = 0.5$ was associated with a decrease in slope b_x^+ downstream of the seal during lake drainage (§6 of the main paper). A closer examination reveals that, for the uplift rate $w(x)$ and parameter values used in our calculations, the downstream slope b_x^+ only decreases slightly (that is, becomes less negative) relatively later during lake drainage for the $\alpha = 0$ case (figure 3, which corresponds to figure 12 of the main paper).

This occurs because the shock that breaches the initially smooth lake seal forms at the seal location itself. As lake drainage proceeds, increases in flux q do cause characteristics to migrate at

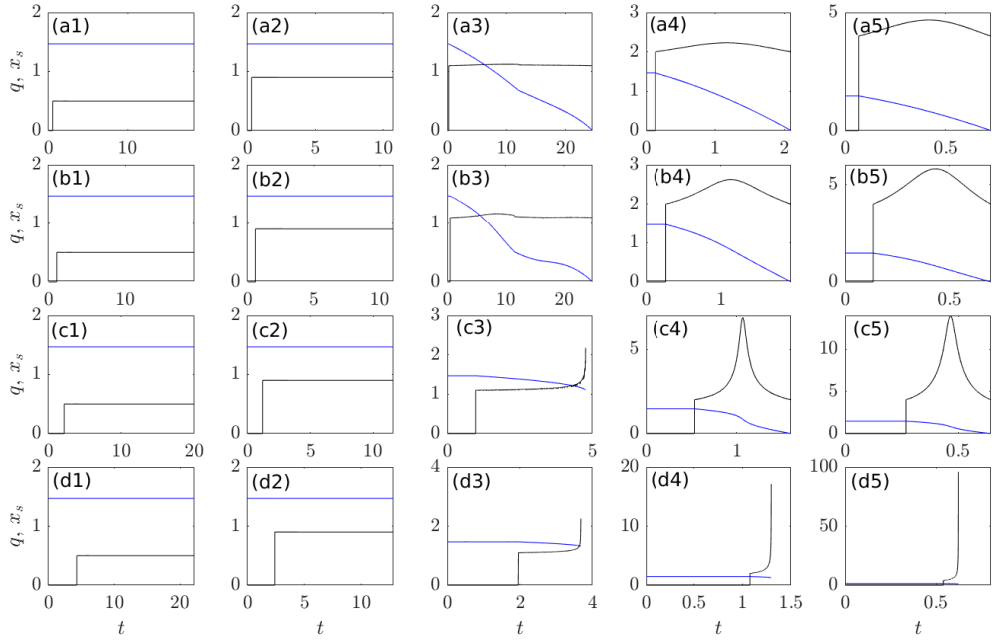

Figure 2: Solutions for $\alpha = 0$: Time series of $q(t)$ and $x_{\rm m}(t)$ (as shown in e.g., panels c of figure 10 of the main paper) for different combinations of γ and Q. $\gamma = 0.5$ (row a), 1 (row b), 2 (row c) 4 (row d) and $Q = 0.5$ (column 1) 0.9 (column 2) 1.1 (column 3) 2 (column 4) and 4 (column 5). The solutions in figure 10 are shown in panels c3 and c4 respectively. The critical water input for seal breaching is $Q = U = 1$, in agreement with the results here.

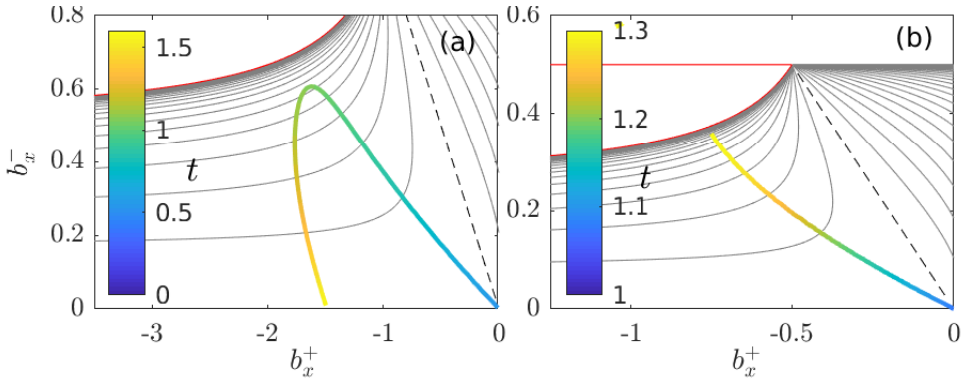

Figure 3: Same as figure 12 of the main paper but showing solutions with $\alpha = 0$ as in figure 2, a) panels c4 and b) d4, overlaid on the appropriate version of figure 6(b). Note that each 'orbit' starts at the origin here, since the shock forms at the smooth lake seal, with initially vanishing up- an downstream slopes.

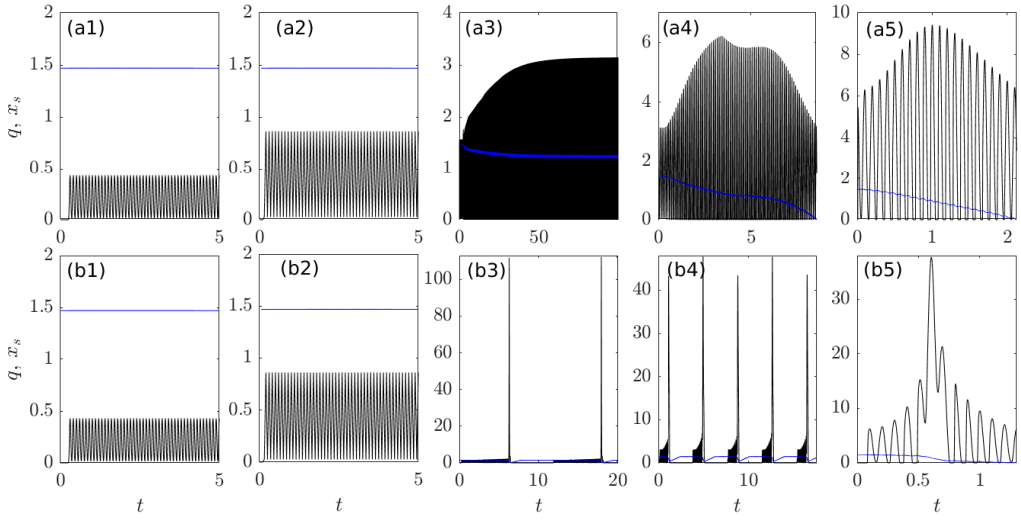

Figure 4: Solutions for $\alpha = 0.5$: Time series of $q(t)$ and $x_m(t)$ for different combinations of γ and Q_0. $\gamma = 2$ (row a) and 8 (row b) and $Q_0 = 0.2185$ (column 1), 0.4371 (column 2) 0.8634 (column 3), 1.570 (column 4) and 3.140 (column 5).

a faster rate $U - q$ and therefore to experience less steepening as already described above. These characteristics however originate further downstream from the smooth lake seal, and therefore start with a steeper slope because the initial conditions dictate as much. The initially steeper slope dominates and downstream slopes initially continue to steepen at the backward-migrating shock, and only flatten slightly just before lake drainage is complete, see figure 3(a). That is not to say that periodic drainage is impossible for $\alpha = 0$, but only that we have not found any examples in which it occurs for the particular uplift function w and initial conditions $b = s$ used here.

5.2 Time-dependent water supply

The results in the main paper assume a steady water input Q to the lake. This is significant since the time scale $[t] = [x]/[U]$ can be quite long compared with a single year, and hence the annual melt cycle: for $[x] = 1$ km and $[U] = 100$ m yr^{-1}, $[t]$ equates to ten annual cycles.

In figures 5, we recompute solutions for the same uplift function $w(x)$ as in the main paper,

$$w(x) = U\left\{b_{0x} - 2b_1\lambda(x - x_0)\exp\left[-\lambda\left(x - x_0\right)^2\right]\right\}$$

with $x_0 = 1.5960$, $b_1 = \lambda = 1$, $b_{0x} = -0.25$ and $U = 1$. We again use a steady-state initial condition satisfying $Ub_{in,x} = w$. We do so with an oscillating water input $Q(t) = Q_0(1 + \cos(\omega t))$, restricting ourselves to $\alpha = 1/2$. We use a relatively large $\omega = 20\pi$. With rapid oscillations in ω, it is natural to expect that the evolution of b at least qualitatively replicates the dynamics for a constant Q given by a nonlinear average over the time-dependent $Q(t)$, since we expect little change in b over a single water supply cycle.

This is largely borne out by our numerical results (figure 5), which show near-steady water levels for low Q_0, and either complete lake drainage for larger Q_0 and moderate storage capacity γ, or oscillatory lake drainage for moderate Q_0 and larger γ. Note that seal lake drainage occurs at larger mean water input Q_0 when water input is oscillatory. This can presumably be attributed to $M = (-q^{1-\alpha}b_x)^{3/(3-\alpha)}$ used in the main paper being concave in q: as a result, the time average of M for a fixed slope $-b_x$ is smaller for variable q than for fixed q with the same average by Jensen's

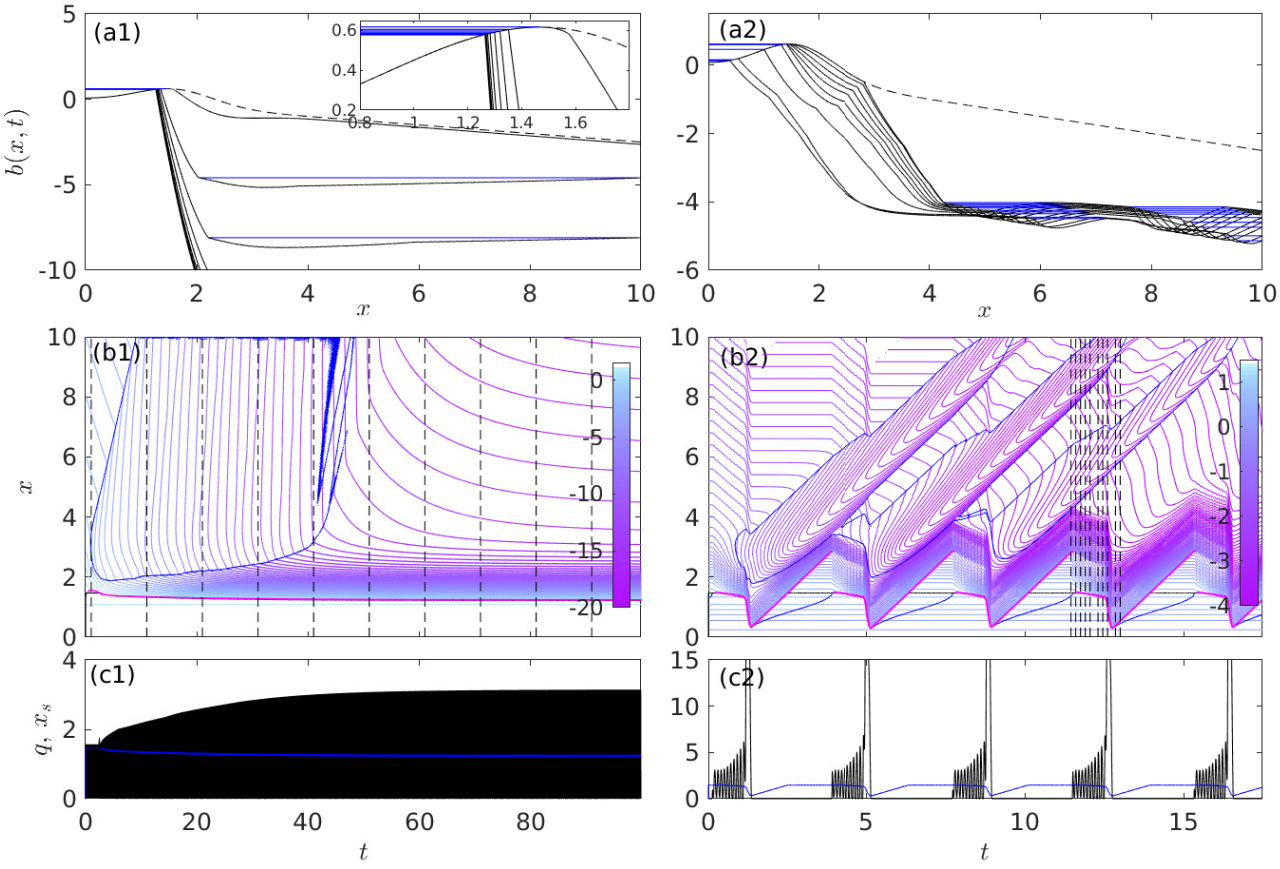

Figure 5: Solutions for $\alpha = 0.5$: $\gamma = 2$, $Q_0 = 1.570$ (column 1) and $\gamma = 8$, $Q_0 = 3.140$ (column 2). Same plotting scheme a figure 7 of the main paper. The inset in panel a1 shows details of the shock at the seal settling into a near-steady position.

inequality. A larger mean flux q is required to produce the same amount of incision if the flux varies in time.

Panel a3 of figure 4 is notable because it does not reproduce any of the cases in figure 10 of the main paper we observe partial seal incision and lake drainage, but with the seal eventually settling into a near-steady state, performing small-amplitude oscillations about some mean at the forcing frequency ω. This case is illustrated in more detail in column 1 of figure 5. Here a shock forms downstream of the initial, smooth seal and then migrates backwards as in the solutions with constant Q. After a short distance, it ceases to incise into the seal much further: as water input into the lake drops off during the cycle, flux q is reduced, allowing uplift to become dominant near the seal and potentially even seal the lake entirely again if uplift is fast enough for seal height to rise faster than water levels in the lake. Over multiple cycles, this can lead to the downstream side of the seal continuing to steepen while the seal itself does not migrate backwards. Note that this occurs even though the mean water input into the lake Q_0 is big enough to cause complete drainage of the lake with steady flow ($\omega = 0$), compare panel a3 of figure 4 here and panel c4 of figure 10 in the main paper.

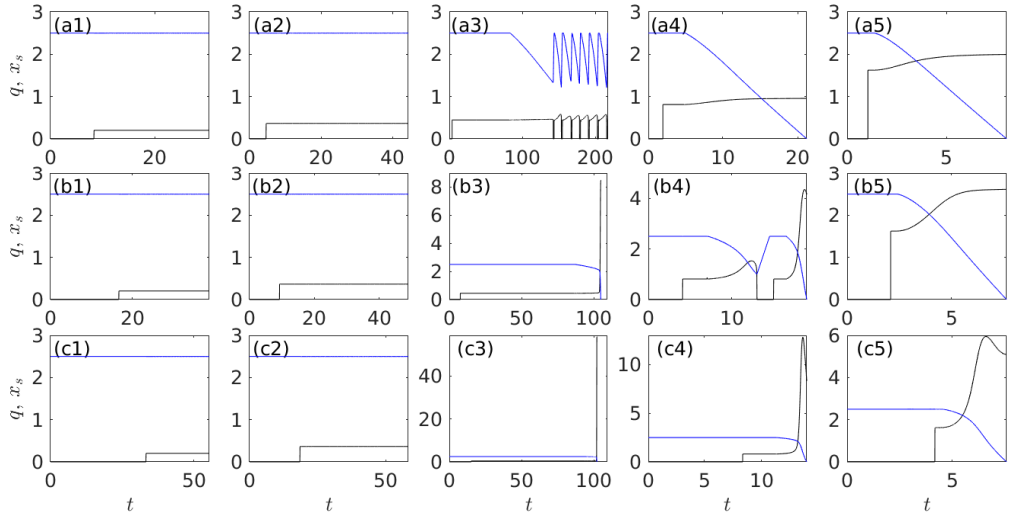

Figure 6: Solutions for $\alpha = 0.5$: Time series of $q(t)$ and $x_m(t)$ for different combinations of γ and Q_0. $\gamma = 1$ (row a), 2 (row b) and 4 (row c), as well as $Q = 0.2031$ (column 1), 0.3655 (column 2) 0.4467 (column 3), 0.8122 (column 4) and 1.6245 (column 5). Note that there is very rapid full lake draiange in panels b3 and c3 at the end of the interval shown. The critical value Q_c for seal incision for the uplift function used here is 0.4062.

5.3 Non-smooth lake bottom

In the main paper, we employed a single uplift function $w(x)$, creating a smooth Gaussian bump in the unincised ice surface s given by $Us_x = w$, superimposed on a gentler, constant downward slope. The resulting lake has an identifiable bottom at $x = 0$ where $s_x = 0$, and this has consequences for the termination of lake drainage (section 4.3 of the main paper) as the upstream slope b_x^- of a shock that incises the lake seal eventually decreases as the low point of the lake is approached.

In this section, we consider an alternative uplift function that generates a lake seal upstream of which the ice surface approaches a constant upward slope:

$$w(x) = -U\frac{x - x_0}{\sqrt{1 + (x - x_0)^2}}, \tag{61}$$

giving rise to a hyperbolic unincised ice surface (dashed line figure 7, panels a1 and a2)

$$s(x) = -\sqrt{1 + (x - x_0)^2}.$$

In the computations reported here, we put $x_0 = 2.5$. An ice surface profile of this type cannot describe a lake on an ice sheet, since we expect the ice surface to continue smoothly upstream of the lake on an ice sheet; instead, the type of lake described by the uplift function in (61) could occur at the confluence of two valley glaciers, or a similar marginal setting.

Again we use constant Q and γ in each computation. The key observation in our results is that oscillatory solutions become much less common, and (near) periodic ones even more so. Figure 6 is the equivalent of figures 10–11 of the main paper, while figure 7 is the equivalent of figure 8 of the main paper.

The only oscillatory behaviour we see is in panels a3 and b4 of figure 6, with only the former appearing to be periodic (close inspection reveals that the oscillation is not perfectly periodic, but of slowly growing amplitude). All other cases either maintain a smooth seal (for the cases where

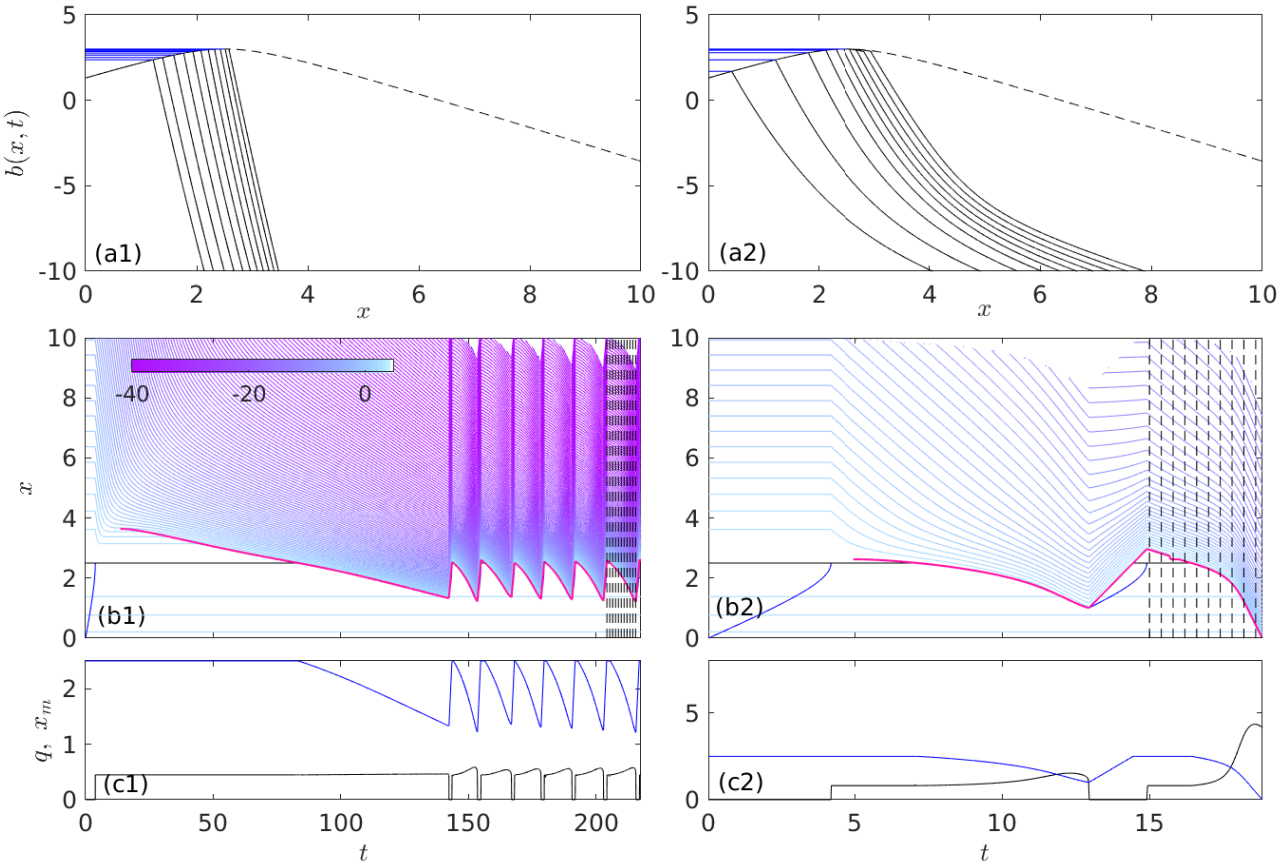

Figure 7: Solutions for $\alpha = 0.5$: $\gamma = 1$, $Q = 0.4467$ (column 1) and $\gamma = 2$, $Q = 0.8122$ (column 2), same basic plotting scheme as figure 7 of the main paper. Contour intervals in panels b1 and b2 are 0.5.

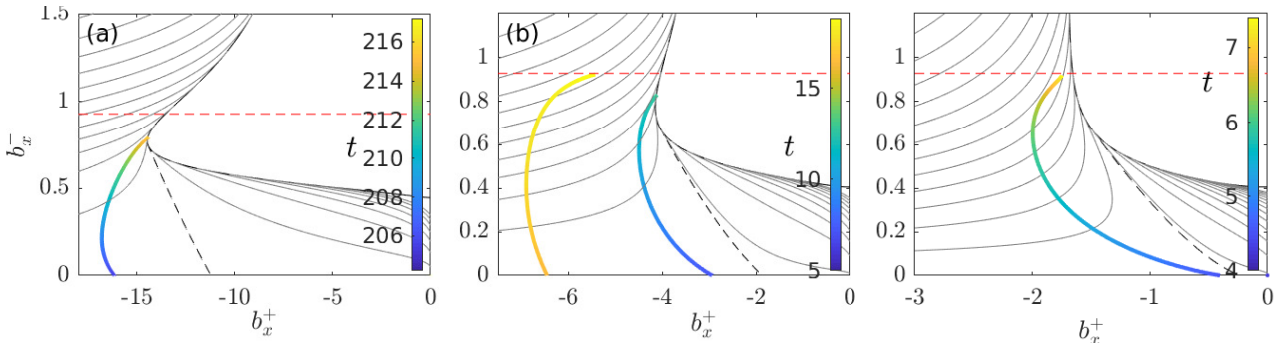

Figure 8: The equivalent of figure 12 of the main paper for the solutions in figure 6 here: 'orbits' of (b_x^+, b_x^-) at the shock that breaches the seal, superimposed on contour lines of q as a function of b_x^- and b_x^+. The dashed red line corresponds to the slope b_x^- at the upstream end of the domain. If an orbit reaches this line, lake drainage is complete. Shown are the solutions in (a) figure 6a3, or column 1 of figure 7 (b) figure 6b4, or column 2 of figure 7, and (c) figure 6b5, corresponding to non-oscillatory, complete lake drainage. Note that unlike figure 13 of the main paper, complete lake drainage does *not* correspond to the upstream slope b_x^- vanishing, but to $b_x^- = 0.9285$. Note that in the case of repeated oscillations, the downstream slope b_x^+ only decreases marginally in the later stages of each drainage cycle (panel a here), in marked contrast to panel a of figure 13 of the main paper.

$Q < Q_c = 0.4062$) or lead to complete lake draiange (with the examples in panels b3 and c3 being difficult to discern because the final drainage at the end of the plots is extremely rapid).

The two oscillatory examples are shown in more detail in figure 7. Comparing these with the corresponding figure 8 of the main paper, it should be clear that, for the case of repeated oscillations in column 1, the solution in figure 7 here involves the same shock (magenta curve) repeatedly incising into the seal. while in figure 8 of the main paper, a new shock is formed in each drainage cycle, ensuring perfect periodicity (see figure 14 of the main paper).

We can repeat the visualizations of figures 13 and 14 of the main paper for the 'hyperbolic' uplift function. The most obvious difference between figure 8 here and figure 13 of the main paper are that downstream slope b_x^+ decreases only slightly and upstream slope b_x^- inevitably does not decrease at all before termination of drainage at the boundary of the blank zero-flux region. In addition, complete lake drainage does not correspond to upstream slope b_x^- vanishing, but to $b_x^- = 0.9285$.

The equivalent of figure 12 in the main paper for the nearly periodic solution of figure 6a3 (or column 1 of figure 7) is shown in figure 9. We see that lake termination does involve characteristics with less steep slopes b_x^+ arriving at the seal late in the drainage cycle, but the reason for this appears to be less a more rapid transit across the smooth seal location $\bar{x}_m$ as in the main paper, but simply the fact that these characteristics start out with less steep slopes (panel a of figure 9). In addition, figure 9 underlines the fact that the same shock incises into the seal during repeated drainage cycles, unlike the smooth-bottomed lake example of the main paper.

References

A.C. Fowler, 2011. *Mathematical geoscience*. Vol. **36** of *Interdisciplinary Applied Mathematics*. Springer-Verlag, Berlin.

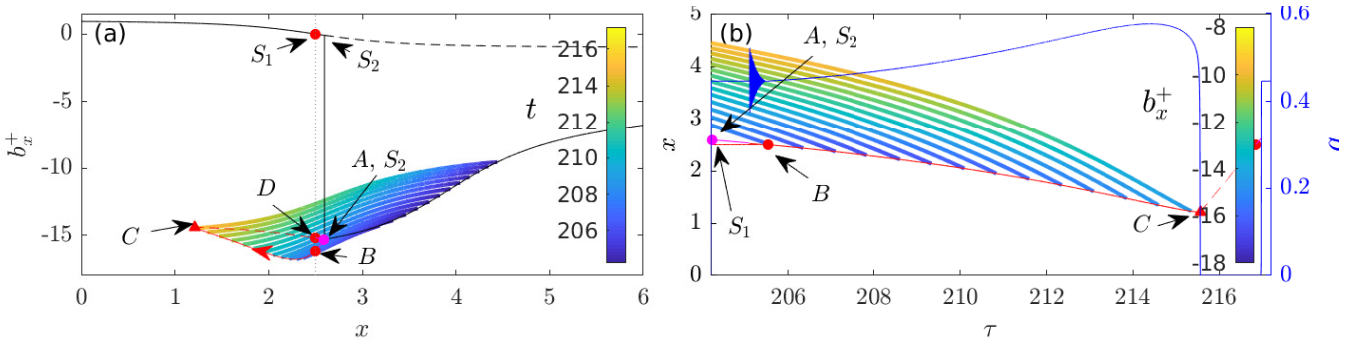

Figure 9: The equivalent of figure 13 of the main paper for the solutions in figure 7, column 1 here, same plotting scheme as figure 14 of the main paper. Note that the 'new' shock A is in fact the old shock S_2, unlike the situation in figure 14 of the main paper. Note also that the later characteristics to arrive at the shock are not flattened significantly relative to the early ones, but simply start with a larger (less negative) initial b_x.

M.H. Holmes, 1995. *Introduction to Perturbation Methods*. Vol. **20** of *Texts in Applied Mathematics*. Springer-Verlag, New York.

J. Kingslake, F. Ng, and A. Sole, 2015. Modelling channelized surface drainage of supraglacial lakes. *J. Glaciol.*, **61**(225), 185–199.